TEXAS A&M AGRILIFE RESEARCH & EXTENSION

COTTON ENTOMOLOGY
RESEARCH REPORT 2020

TECHNICAL REPORT 21-4

TEXAS A&M AGRILIFE RESEARCH, PATRICK J. STOVER, DIRECTOR
THE TEXAS A&M UNIVERSITY SYSTEM, COLLEGE STATION, TEXAS

COTTON ENTOMOLOGY PROGRAM

RESEARCH ACTIVITY ANNUAL REPORT

2020

SUBMITTED TO:

PLAINS COTTON IMPROVEMENT COMMITTEE
PLAINS COTTON GROWERS, INC.

JAROY MOORE, CENTER DIRECTOR
TEXAS A&M AGRILIFE RESEARCH-LUBBOCK

BY:

Dr. Megha N. Parajulee
Professor, Faculty Fellow, and Texas A&M Regents Fellow
Texas A&M AgriLife Research Cotton Entomology Program
1102 East Drew Street, Lubbock, Texas 79403
Phone: (806) 746-6101; Fax: (806) 746-6528
Email: m-parajulee@tamu.edu

PARTICIPANTS

ABDUL HAKEEM, Texas A&M AgriLife Research-Lubbock

BEAU HENDERSON, Texas A&M AgriLife Research-Lubbock

BLAYNE REED, Texas A&M AgriLife Extension Service- Plainview

CASEY HARDIN, Texas A&M AgriLife Research-Halfway

DANIELLE SEKULA-ORTIZ, Texas A&M AgriLife Extension Service- Weslaco

DANNY CARMICHAEL, Texas A&M AgriLife Research-Lamesa

DOL P. DHAKAL, Texas A&M AgriLife Research-Lubbock

JANE DEVER, Texas A&M AgriLife Research-Lubbock

JIM BORDOVSKY, Texas A&M AgriLife Research-Lubbock

KATIE LEWIS, Texas A&M AgriLife Research-Lubbock

KERRY SIDERS, Texas A&M AgriLife Extension Service- Levelland

MEGHA PARAJULEE, Texas A&M AgriLife Research-Lubbock

MICHAEL BREWER, Texas A&M AgriLife Research-Corpus Christi

MICHAEL TOEWS, University of Georgia, Tifton

RAJAN GHIMIRE, New Mexico State University, Clovis

STEPHEN BILES, Texas A&M AgriLife Extension Service- Port Lavaca

SUHAS VYAVHARE, Texas A&M AgriLife Extension Service-Lubbock

WAYNE KEELING, Texas A&M AgriLife Research-Lubbock

FUNDING AND LOGISTICAL SUPPORT

USDA NIFA, Cotton Incorporated Core Program, CI State Support Committee, Texas A&M AgriLife Research, Texas A&M AgriLife Extension Service, Plains Cotton Improvement Program

TABLE OF CONTENTS

Introduction

Plains Cotton Growers, Inc. (PCG) has been a strong supporter of cotton insect research and extension activities in west Texas for many years. Most notably, PCG was instrumental in securing state funds for the Boll Weevil Research Facility at the Lubbock Center, and provided both financial and political support to conduct boll weevil biology and ecology research even before the boll weevil became a significant economic pest of the High Plains region. After the initial entry of the boll weevil into the eastern edge of the High Plains, PCG promoted and along with USDA-APHIS administered the boll weevil diapause suppression program involving a team effort that continued to include Texas A&M University. PCG also supported Texas Cooperative Extension (now Texas A&M AgriLife Extension Service) efforts to annually evaluate the diapause suppression program, conduct applied research trials to develop boll weevil management practices that would enhance the diapause suppression program's efforts, and in the 1990s supported an annual survey of High Plains overwintering sites and grid trapping of cotton across the High Plains area. The team effort of PCG, Texas A&M AgriLife Research and AgriLife Extension Service over several decades has resulted in a comprehensive understanding of boll weevil ecology and behavior. Under the strong and cooperative leadership of PCG, the boll weevil eradication program for the High Plains area progressed much more rapidly than anticipated. Now, the successful boll weevil eradication program has eliminated the boll weevil from this region for nearly two decades.

With a successful boll weevil eradication program and increased adoption of the transgenic *Bt* technology (now >70%), the cotton insect research and extension program focus has changed considerably during the last 20 years. Our current research/extension focus is on developing ecologically intensive strategies for cotton pest management, including crop phenology, cultivar, non-crop habitat, irrigation, and fertility management towards reducing insect pest pressure. Our research has demonstrated the need for continuing investigation of basic behavior and life patterns of insects while having a strong field-based applied research to bridge the gap between basic, problem-solving science and producer-friendly management recommendations. We have assembled a strong group of people to work as a team to examine multiple disciplines within the broad theme of Cotton IPM. We invest considerable time and manpower resources in investigating the behavior and ecology of major cotton pests of the High Plains with the goal of developing management thresholds based on cotton production technology and economics, with particular focus on limited water production system. Our Program has successfully leveraged research funds based on the funding provided by PCIC to support our research effort. We are excited about and greatly value our Cotton Entomology research and extension partnerships with multidisciplinary scientists at the Texas A&M AgriLife Research Center, together with area IPM agents in the region, to continue this partnership as we challenge ourselves to deliver the best cotton insect-pest management recommendations to our Texas High Plains producers. Together, we have maintained the Texas High Plains area as a characteristically low cotton insect-pest prevalence region in the U.S. cotton belt.

EFFECT OF NITROGEN FERTILITY ON COTTON CROP RESPONSE TO SIMULATED COTTON FLEAHOPPER AND LYGUS DAMAGE

M.N. Parajulee, D. P. Dhakal, A. Hakeem, and K. L. Lewis

Objective: The objective was to evaluate the effect of artificial injury to cotton squares mimicking acute cotton fleahopper damage under variable nitrogen application rates on cotton fiber yield and quality.

Methodology: A high-yielding cotton cultivar, NG3930B3XF, was planted at a targeted rate of 54,000 seeds/acre on May 21, 2020. The experiment was laid out in a split-plot randomized block design with five nitrogen fertility rate treatments (0, 50, 100, 150, and 200 lb N/acre) applied for 18 years as main plots (16-row plots) and three fruit loss treatments (artificial cotton square injury treatment mimicking acute cotton fleahopper infestation, 20% boll removal treatment to mimic late-season Lygus infestation, and control) as sub-plots with four replications (total 60 experimental units). Within each of the five main-plot treatments included pre-bloom side-dress applications of N augmentation using a soil applicator injection rig on July 30, 2020. Pre-treatment soil samples (consisting of three 0 to 12 and 12 to 24-inch depth soil cores each) were collected from each of the 20 main-plots on June 12, 2020. Ten leaves per plot were collected twice (August 13 and September 17) for leaf dry weight and nitrogen analysis. Within each main-plot, three 10-ft. sections of uniform cotton were flagged in the middle two rows, each receiving hand removal of 100% cotton squares three weeks into squaring, 20% bolls removed from top canopy of the plants at crop cut-out or control (no square or boll removal). Treatment plots were hand-harvested on October 19 for lint yield and fiber analysis.

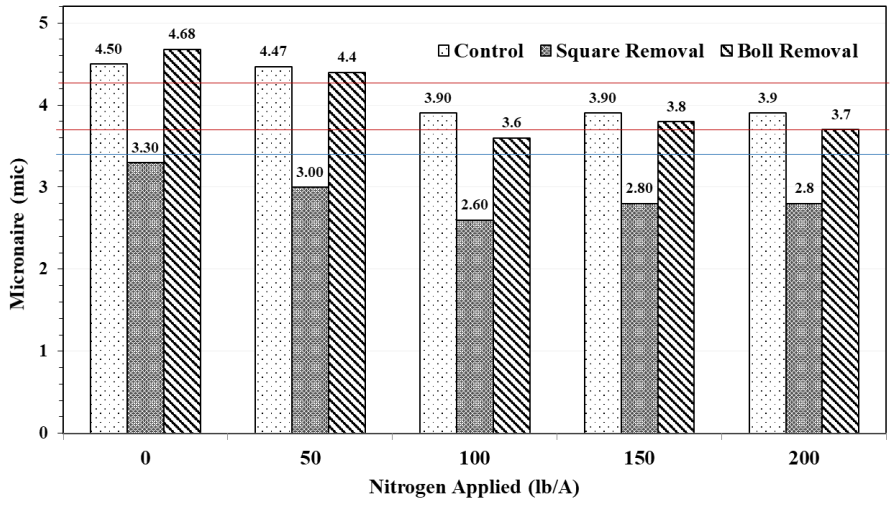

Fig. 1. Lint micronaire values affected by simulated cotton fleahopper and Lygus damage through artificial square and boll removal across variable N rates.

Results: Significantly higher soil residual nitrogen was recorded from plots that received high rates of soil N augmentation in preceding 17 years than control plots. Lint yield did not significantly vary across simulated insect treatments or N augmentation treatments, owing to considerable variation in data due to poor stand establishment and mid-season drought. Nevertheless, the lint quality, measured in terms of micronaire values, was significantly impacted by the simulated cotton fleahopper damage. Early season square removal lowered the micronaire values to a discount range regardless of N level, whereas late season 20% boll removal did not significantly impact the micronaire values (Fig. 1). Micronaire values in both control and boll removal treatments were in the base range at lower N rates and premium range at 100 lb/A and higher N rates.

TITLE:

Cotton yield response to simulated cotton fleahopper and western tarnished plant bug infestations as influenced by irrigation level and cultivar treatments, Lamesa, TX, 2020.

AUTHORS:

Megha Parajulee – Professor, Faculty Fellow, and Regents Fellow
Abdul Hakeem – Assistant Research Scientist
Dol Dhakal - Research Associate
Wayne Keeling - Professor

MATERIALS AND METHODS:

Plot Size:	4 rows by 300 feet, 3 replications
Planting date:	May 20
Fertilizer in-season:	120-0-0
Cultivars:	PHY 350 W3FE and ST 4946 GLB2
Irrigation:	Low / High Preplant 3.9” / 3.9” In Season 5.1” / 10.1” Total 9.0” / 14.0”
Herbicides:	Prowl H_2O 3 pt/A+Roundup 24 oz/A – pre-planting (April 21) Gramoxone 32 oz/A+Caparol 32 oz/A – post-planting (May 21) Roundup 32 oz/A (June 12) Roundup 32 oz/A+Dual Magnum 20 oz/A (July 7)
Treatments:	Three treatments included c*ontrol*, *manual removal of 100% squares three weeks into squaring (July 15) to time cotton fleahopper susceptible stage, and removal of 20% bolls from the top of the plant to simulate Lygus infestation (August 21).*
Harvest date:	October 13, 2020 (hand-harvested)

Effect of manual removal of early-stage versus late-stage fruits was evaluated on two cotton cultivars, PHY 350 W3FE and ST 4946 GLB2, as influenced by two irrigation (low and high) water levels. The experiment comprised of two water levels, two cultivars, and three simulated fruit loss events [control, pre-flower 100% square loss mimicking the cotton fleahopper injury-induced loss, and 20% small bolls (<3 cm diameter) loss mimicking the Lygus boll injury-induced small fruit abortion at cut-out], replicated three times, totaling 36 plots. The test plots were monitored for the occurrence of any other insects, but no such occurrences were observed during the growing season.

RESULTS AND DISCUSSION:

Combined over two cultivars and three insect simulation treatments, significantly higher lint yield was recorded from ‘high’ water regime (936 lb/acre) compared to that in ‘low’ water regime (725 lb/acre). However, no significant difference in lint yield was recorded between insect simulated (cotton fleahopper or Lygus) and control plots regardless of the water regime (Fig. 1). Although

not significant, late season fruit removal mimicking Lygus injury reduced lint yield by about 200 lb/A compared to that for early season square removal at both irrigation regimes (Fig. 1), indicating a greater pest risk at cut-out than pre-flower fruit abortion. While Lygus simulation consistently reduced lint yield across all irrigation water level X cultivar combinations, ST 4946 GLB2 at high water treatment showed the most impact (Fig. 2). Also, the yield performance of ST 4946 GLB2 much more sensitive too water level than PHY 350 W3FE (Fig. 2).

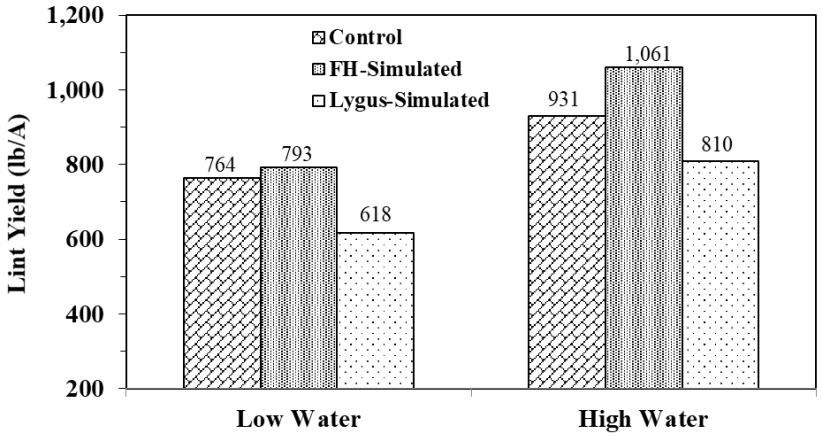

Figure 1. Average lint yield under low and high irrigation regimes following cotton fleahopper and Lygus infestation simulation versus control, Lamesa, Texas, 2020.

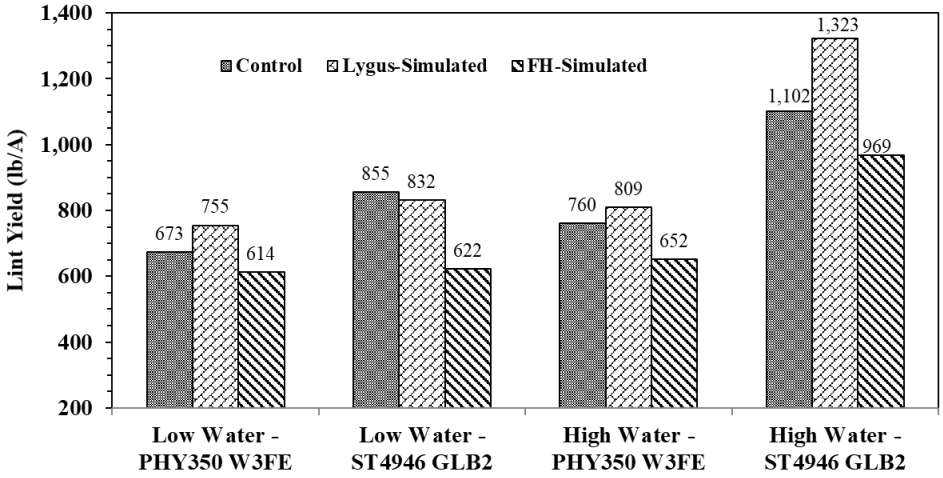

Figure 2. Average lint yield influenced by simulated cotton fleahopper versus *Lygus*-induced fruit removal in two cotton cultivars under low and high irrigation regimes, Lamesa, Texas, 2020. Average values were not statistically significant due to high variation in data.

Averaged over two cotton cultivars, early-season square removal resulted in increased micronaire values at low irrigation regime, reaching to the discount range (Fig. 3). The effect of late-season simulated *Lygus*-induced fruit removal did not significantly influence the lint micronaire. The increased irrigation water level (high water regime) improved micronaire values in cotton cultivar PHY 350 W3FE the micronaire was generally unchanged across cultivar X irrigation treatment combinations (Fig. 4).

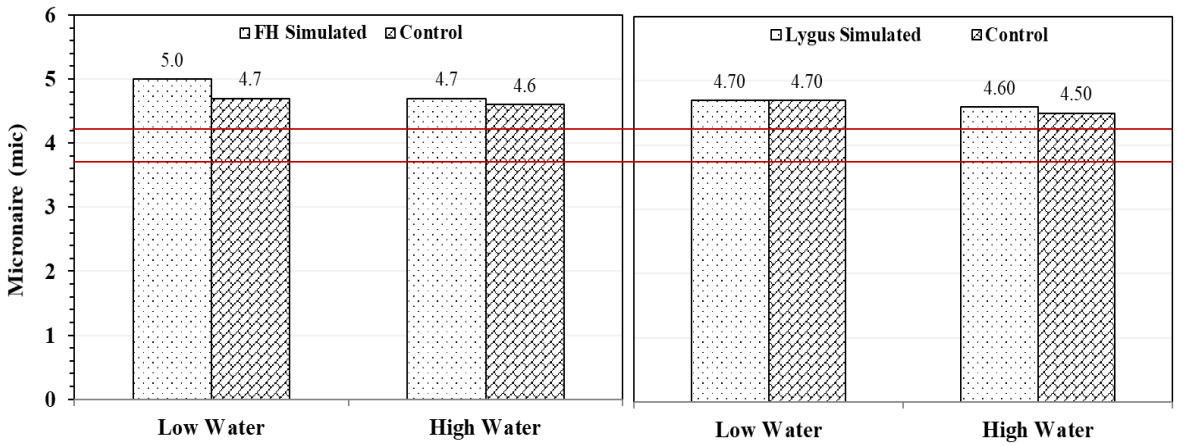

Figure 3. Average micronaire values influenced by early-season simulated cotton fleahopper damage (left) and simulated *Lygus*-induced fruit removal in late season averaged over two cotton cultivars under low and high irrigation regimes, Lamesa, Texas, 2020. The area enclosed by two red lines (3.7-4.2) indicates the microaire values for premium quality cotton lint.

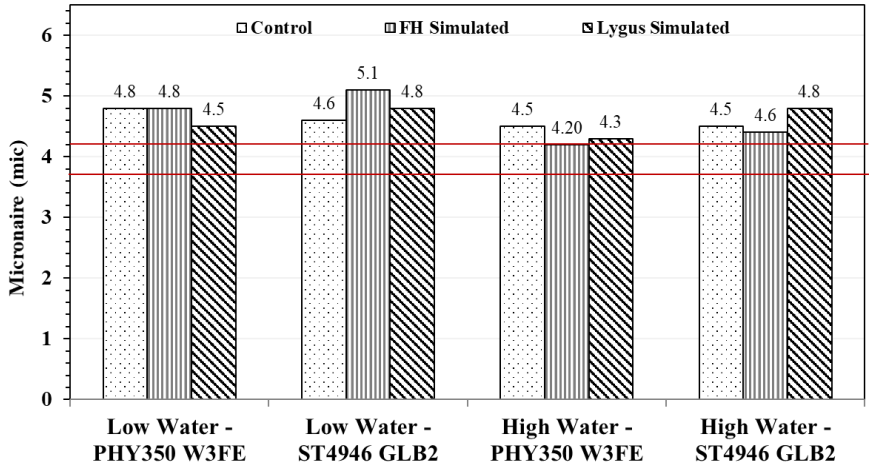

Figure 4. Average micronaire values influenced by early-season simulated cotton fleahopper damage and simulated *Lygus*-induced fruit removal in late season in two cotton cultivars under low and high irrigation regimes, Lamesa, Texas, 2020. The area enclosed by two red lines (3.7-4.2) indicates the micronaire values for premium quality cotton lint.

Cotton fleahopper susceptibility and compensatory potential of three distinct phenological stages of pre-flower cotton in water-deficit production scenario

Cotton Incorporated – Core Program
Project Number: 20-246

Megha N. Parajulee
Texas A&M AgriLife Research and Extension Center, Lubbock, Texas

Project Summary

The recent increase in limited-irrigation cotton production in the Texas High Plains has demanded development of pest management strategies at low-input production system. Our current understanding is that cotton fleahoppers can be injurious to cotton during 3-weeks of squaring until about the appearance of first flower. That may warrant possible management of cotton fleahoppers up to three discrete stages of cotton prior to flowering as stated earlier. Impact of cotton fleahoppers on pre-squaring stage, especially when fleahoppers migrate to cotton prior to the occurrence of visible squares, and late squaring/first-flower stage is not quantified. Our earlier work on cotton fleahopper compensation studies suggest that cotton plants can tolerate up to 20% fruit loss. This project aims to investigate the growth and fruiting response of cotton after cotton fleahopper induced square loss at three discrete cotton fleahoper susceptible stages of cotton under deficit-irrigation scenario. The specific objectives of the study were to 1) quantify the damage potential of cotton fleahopper (feeding injury and/or square abortion) at square initiation (prior to visible squares), 1-2-square, and 4-5-square stages of cotton under dryland, deficit irrigation versus full irrigation, 2) determine cotton growth parameters and fruiting profiles as influenced by cotton fleahopper injury at three discrete cotton fleahoper susceptible stages of cotton under deficit-irrigation scenario, and 3) quantify cotton compensatory potential following cotton fleahopper induced square loss under phenological stage x irrigation treatments.

This study is expected to generate a significant amount of data to elucidate the damage potential of cotton fleahoppers at three discrete cotton fleahopper susceptible stages under two drought-stress conditions, including low/supplemental irrigation (drought stress) and full irrigation (no drought stress), and cotton's response to cotton fleahopper injury under each production scenario. The data regarding how the cotton fleahopper injury x drought-stress conditions impact cotton performance at three discrete phenological stages will be useful in making management decisions based on economic models.

Cotton fleahopper infestation at pre-squaring stage reduced cotton lint yield across all three irrigation treatments, although significant only under dryland condition. It is plausible that fleahoppers fed on growing terminals and likely damaged the invisible squares which ultimately reduced the lint yield. Cotton fleahoper infestation also impacted fiber quality, with improved micronaire values under full irrigation. The 2020 study clearly suggests that there is an apparent interaction between fleahopper-induced injury to cotton and irrigation water availability for plants to overcome the injury effect, thereby influencing the lint yield and fiber quality. Additional 2-3 years of studies will provide more insight into these results.

Introduction

The cotton fleahopper, *Pseudatomoscelis seriatus* (Reuter), is a significant economic pest of cotton in the Texas High Plains. Injury by cotton fleahoppers to squaring cotton often causes excessive loss of small squares during the early fruiting period of plant development (first 3 weeks of squaring). There has been some evidence that cotton fleahoppers also infest pre-squaring cotton plant terminals, perhaps when squares are developing on the plant. Both adults and immatures feed on new growth, including small squares. Greater damage is observed on smooth leaf varieties than on hirsute varieties, which may extend the susceptible period into early bloom, especially under a high-input production regime. Generally, cotton is affected by cotton fleahopper injury from about the fifth true-leaf through first week after initiation of flowering. Squares up to pinhead size are most susceptible to damage, and yield loss is most likely from feeding during the first three weeks of fruiting. Cotton fleahopper damage also delays crop maturity and thus increases the vulnerability of cotton to late season pests such as Heliothine caterpillars and *Lygus* bugs, particularly when natural enemies are destroyed by insecticides directed against cotton fleahoppers.

Predominantly, cotton fleahoppers feed upon pinhead-sized or smaller squares, which results in abortion of these young fruits, thereby impacting yields. While cotton fleahopper feeding preferences serve as a baseline for their management in cotton fields, a detailed understanding of cotton plant responses to fleahopper damage remains unachieved. Because cotton vulnerability to cotton fleahoppers spans over a period of 3-4 weeks, information on acute infestation of cotton fleahopper at phenologically-specific crop stages may help cotton producers make appropriate management decisions in low-input, water-deficit production systems. Cotton plant growth is sensitive to numerous environmental and management input factors, particularly irrigation and cultivar traits. Cotton growth responses to various input factors are well-documented and growth models have been developed. However, the specific cotton plant responses to cotton fleahopper injury at phenologically discrete cotton fleahopper susceptible stages remain uninvestigated. This research project proposes to evaluate the cotton crop growth parameters and lint yield following cotton fleahopper acute infestations at three distinct cotton fleahopper susceptible cotton stages (pre-squaring, 1-2-square stage, 4-5-square stage) under deficit-water versus full-irrigation production regimes.

Methodology

The study was conducted at the Texas A&M AgriLife Research farm in Lubbock. A 5-acre subsurface drip irrigation system has been in place for this study. Main-plot treatments included full irrigation, supplemental irrigation, and dryland. The full irrigation water level was created via 90% replenishment of evapotranspiration (ET) requirement for THP, whereas the supplemental irrigation treatment received 30% ET replenishment. Cotton cultivar DP 1820 B3XF was planted on 18 May 2020. Sub-plot treatments included three discrete phenological stages of cotton that is considered susceptible to cotton fleahopper damage: 1) prior to the occurrence of visible squares on seedling cotton or “pre-square” cotton, 2) cotton at 1-2 visible squares stage or early squaring stage, and 3) cotton with 4-5 squares and close to the occurrence of first flower or late squaring).

Two 3-ft sections of uniform cotton were flagged in the middle two rows of each treatment plot (3 irrigation treatments x 3 phenological stages x 2 insect augmentation treatments x 4 replications =

48 experimental units) for insect treatment deployment. At each phenological stages, 5 cotton fleahopper nymphs per plant versus no fleahopper augmentation as control were deployed in these designated row sections to simulate an acute infestation of cotton fleahoppers.

Woolly croton, a cotton fleahopper weed host, was harvested from locations in and near College Station, Texas, in early February and stored in cold storage until fleahoppers were needed for the study. Conditions conducive to cotton fleahopper emergence were simulated in a laboratory environment in order to induce hatching of overwintered eggs embedded in the croton stems, and emerged cotton fleahoppers were subsequently reared using fresh green beans as a feeding substrate. Cotton fleahopper rearing cages were installed on 20 May and staggered the cage installation throughout June to ensure a continuous supply of cotton fleahopper nymphs for the study. Considerable effort was expended to ensure synchronization of rearing efforts with cotton crop development for optimal release timing for each of the three cotton phenological stages.

A single release nymphal cotton fleahopper was timed to simulate the acute heavy infestation of cotton fleahoppers (3-4 days of feeding) at each stage. This arrangement ensured significant damage on treatment plots to quantify the variation in damage potential as influenced by cotton phenological stage. The actual release dates were 20 June (pre-square), 1 July (early square), and 21 July (late square). The release was accomplished by manually placing second- to third-instar cotton fleahopper nymphs from the laboratory colony onto the terminals of plants in each treatment plot at the rate of 5 nymphs per plant; the control plots received no fleahoppers and were kept fleahopper-free during the entire study period. Because natural infestation of cotton fleahopper was absent at the experimental farm, the control plots received no insecticidal intervention. An insecticide (acephate 97% 6 oz/acre) was used to kill all remaining cotton fleahoppers after the one-week feeding period in all experimental units to ensure complete removal of released cotton fleahoppers. The entire test was kept insect-free for the remainder of the study to isolate the effect of cotton fleahopper injury only.

Data collection included monitoring of flowering patterns, fruit abscission, and plant height. Flower monitoring was initiated on 20 July and conducted every 2-3-day intervals with total of 14 sample dates. Harvest aids Boll'd® 6SL (Ethephon [(2-chloroethyl) phosphonic acid] @ 1 qt//A (boll opener) and Folex® 6 EC (S, S, S-Tributyl phosphorotrithioate) 1 pint/A (defoliant) were applied on 12 October to accelerate opening of matured unopened bolls and begin the defoliation process. Test plots were hand-harvested on 22 October. Hand-harvested yield samples were ginned, and the samples were analyzed for fiber quality parameters (HVI) at Cotton Incorporated.

Results and Discussion

Cotton fleahopper induced square injuries exerted very low level of square abscission (10-15%). Irrigation water level significantly influenced the cotton lint yield, as expected, with significantly higher yield with increased level of irrigation. Averaged across cotton fleahopper augmentation treatments, dryland produced the lowest lint yield (1102 lb/acre), followed by low water (1420 lb/acre), and the highest lint yield was observed under full irrigation (1691 lb/acre) (Fig. 1). Despite low insect injury, cotton fleahopper infestation at pre-squaring stage (before the onset of visible squares) reduced cotton lint yield across all three irrigation treatments, although the value was statistically significant only under dryland condition (Fig. 2). Even though not significant due to high data variation, lint yields were conspicuously reduced in both supplemental and full irrigation

treatments when cotton fleahoppers were augmented at pre-square stage (Fig. 2). It is plausible that fleahoppers fed on growing terminals and likely damaged the invisible squares which ultimately reduced the lint yield. Also, cotton fleahopper infestations at early as well as late squaring (pre-flower) cotton did not reduce lint yield at any of the three irrigation regimes. Figure 2 suggests that cotton compensated or overcompensated (numerically) any fruit loss due to fleahopper-induced injury, ultimately showing no significant effect on lint yield. Early square stage of cotton appeared to be more susceptible to cotton fleahoppers than late squaring cotton under dryland condition; however, irrigated cotton did not show such differential responses. Manual removal of squares (100% squares removed at the time of first flower coinciding with the fleahopper infestation at late squaring stage) significantly reduced the lint yield under dryland condition, but plants compensated the manually removed fruit abscission under both irrigated conditions.

Cotton fleahoper infestation also impacted fiber quality while the plant response to cotton fleahopper injury was influenced by irrigation water level. High water treatment resulted in micronaire values in the premium range for all fleahopper augmentation sub-plot treatments (Fig. 3). Interestingly, lint fiber from the uninfested control plots had micronaire in the premium range, but the micronaire values increased and moved away from premium range to base range for all FH-augmented plots (Fig. 3). All sub-plot treatments resulted in micronaire values at base range under supplemental irrigation. Manual removal of squares resulted in premium micronaire value under dryland and base value under both irrigation regimes. Other fiber quality parameters varied marginally with insect augmentation X irrigation interactions (Table 1). Although a single season data set, the 2020 study clearly suggests that there is an apparent interaction between fleahopper-induced injury to cotton and irrigation water availability for plants to overcome the injury effect, thereby influencing the lint yield and fiber quality. Additional 2-3 years of studies will provide more insight into these results.

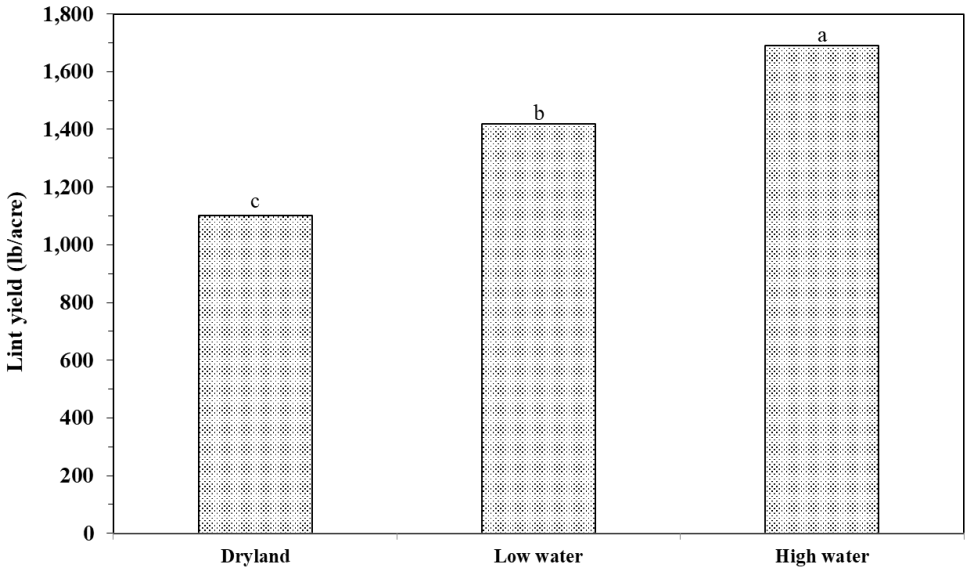

Fig. 1. Average cotton lint yield across cotton fleahopper augmentation treatments under three irrigation water regimes, Lubbock, Texas, 2020. Different lowercase letters indicate treatment means were significantly different from each other.

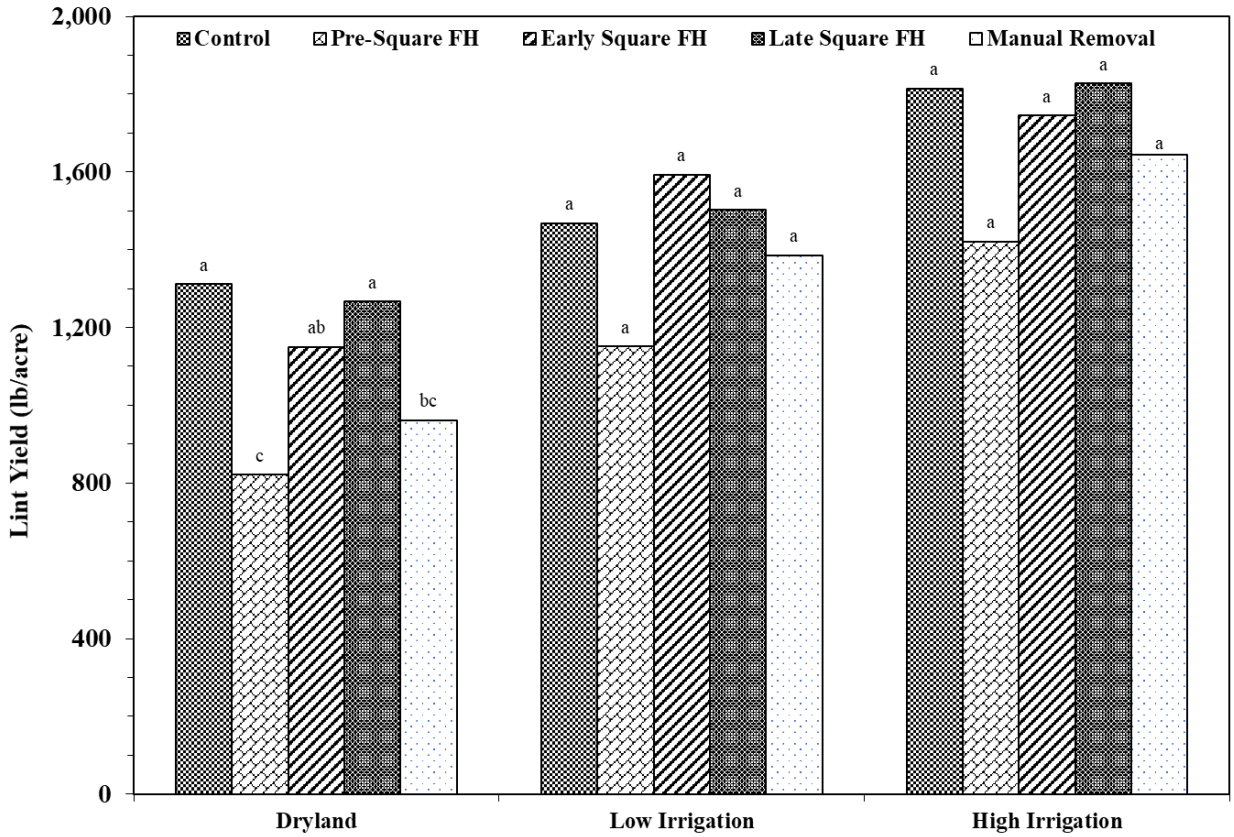

Fig. 2. Cotton lint yield following cotton fleahopper infestations at three cotton phenological stages and manual square removal at first flower under three irrigation water treatments, Lubbock, Texas, 2020. Average values were compared across five treatments within each irrigation treatment; same lowercase letters indicate treatment means were not significantly different from each other. Pre-square FH = fleahoppers augmented prior to the occurrence of visible squares in plants; Early square FH = fleahoppers released at 1-2 visible squares; Late square FH = fleahoppers released when cotton was about to begin flowering; Manual Removal = all visible squares removed from plants at first flower.

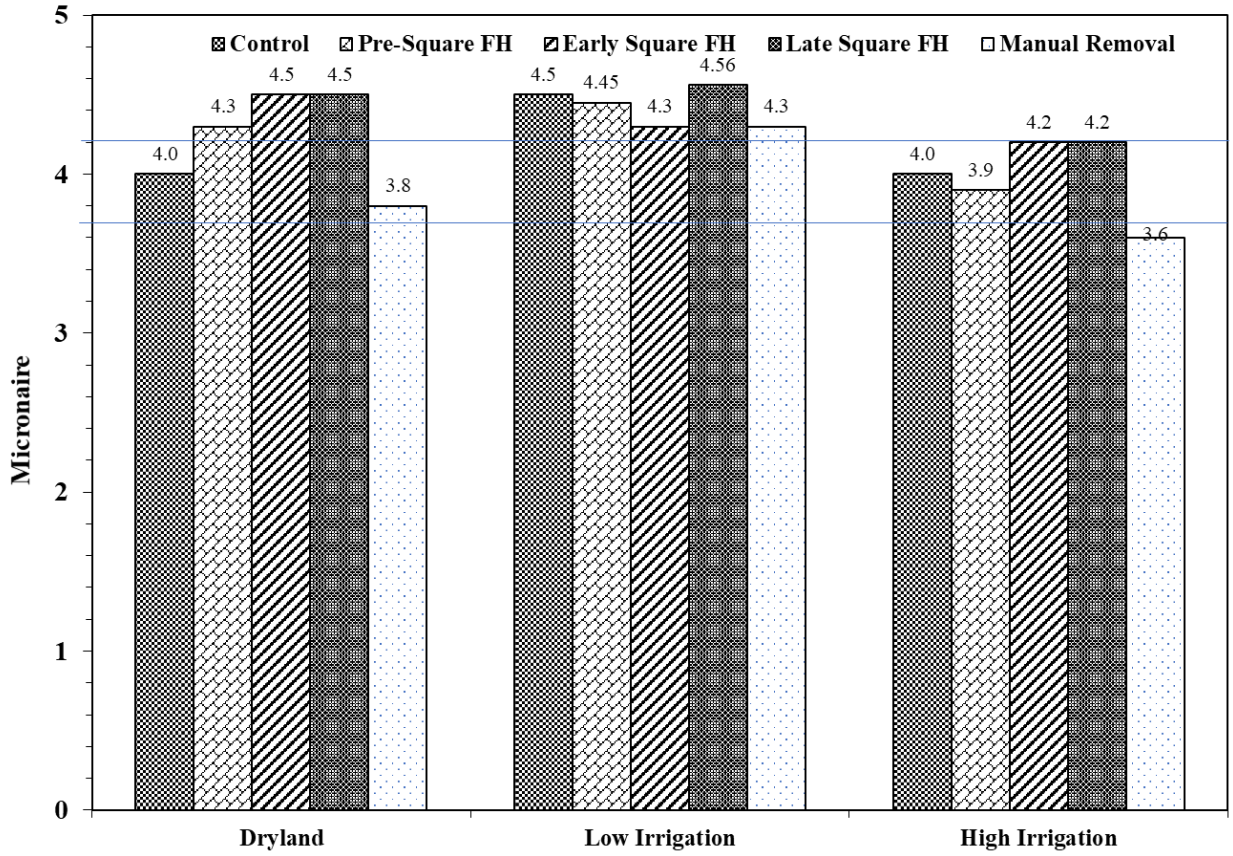

Fig. 3. Cotton fiber micronaire values (units) following cotton fleahopper infestations at three cotton phenological stages and manual square removal at first flower under three irrigation water treatments, Lubbock, Texas, 2020. Two blue lines indicate the region of micronaire values for the premium lint value. Pre-square FH = fleahoppers augmented prior to the occurrence of visible squares in plants; Early square FH = fleahoppers released at 1-2 visible squares; Late square FH = fleahoppers released when cotton was about to begin flowering; Manual Removal = all visible squares removed from plants at first flower.

Table 2. HVI fiber quality parameters influenced by cotton fleahopper augmentation treatments under three irrigation water treatments, Lubbock, Texas, 2020

Fiber Parameters	Irrigation Treatment	Fleahopper Simulation	Uninfested Control	Pre-Square Fleahopper	Early square Fleahopper	Late-square Fleahopper
Micronaire	Dryland	3.08	3.40	4.36	4.51	4.54
Fiber length	Dryland	1.10	1.13	1.14	1.16	1.14
Uniformity	Dryland	80.18	80.43	81.33	81.60	81.50
Strength	Dryland	30.95	31.80	32.13	32.35	32.30
Elongation	Dryland	7.73	7.68	7.65	7.83	7.73
Micronaire	Low	3.43	3.83	4.45	4.30	4.56
Fiber length	Low	1.15	1.16	1.14	1.16	1.16
Uniformity	Low	81.44	81.66	81.55	81.63	82.00
Strength	Low	31.91	31.60	31.88	32.00	31.93
Elongation	Low	7.84	7.99	7.73	7.93	7.85
Micronaire	High	3.00	3.39	3.93	4.24	4.22
Fiber length	High	1.17	1.17	1.20	1.21	1.20
Uniformity	High	80.73	80.94	82.08	82.23	82.60
Strength	High	31.61	31.71	32.15	31.78	31.00
Elongation	High	8.04	8.11	8.28	8.30	8.30

Economic Evaluation of Insect-Pest Management in Water-Deficit Cotton Production

Cotton Incorporated - Texas State Support Committee

Project Number: 18-099TX
PI: Megha N. Parajulee
CO-PIs: Abdul Hakeem, Suhas Vyavhare, Katie Lewis, Wayne Keeling, and Donna McCallister

PROJECT SUMMARY

The Texas High Plains (THP) is a semi-arid region with characteristic low rainfall, with production agriculture supported by limited irrigation or rain-fed. As a result, the cropping system in this region is largely low-input and the producer decision-making in economically profitable input use is a challenge. THP has been facing some significant drought conditions in recent years, including the drought of 2011 that claimed much of the Texas production agriculture, reducing total cotton yield that year by 55%. Drought conditions ensued the next 3 years that disproportionately depleted the underground water, significantly shifting the cotton production outlook in THP to even more low-input with dryland acreage reaching to >65%. The shift in cotton production system due to devastating droughts in an already semi-arid region has altered our input resources, cultivars, and management practices. Low cotton market price, increased nitrogen fertilizer price, and reduced water availability have forced farmers to move toward reorganizing available input resources to sustain their production enterprise. Thus, transitioning to the new crop production reality via developing economic data-based input management practices has become our priority to sustain producer profitability.

The objectives of this project were to: 1) quantify the impact of single (thrips or cotton fleahoppers) versus multiple (thrips and cotton fleahoppers sequentially) pest infestations on cotton lint yield and fiber quality under three irrigation water regimes (water-deficit treatments), and 2) develop a dynamic optimization economic model that maximizes the net returns from management of single versus multiple pest infestations under water-deficit crop production conditions. Thus, the scope of this proposed work entails integrating production practices and pest management options under numerous cotton management scenarios (15 total scenarios) and the management options would be developed based on breakeven value and net return of each option for farmers to choose depending on the availability of water resources on their farms.

Thrips and fleahoppers impacting cotton production risks were evaluated in 2018, 2019, and 2020 with five combinations of single versus sequential infestations under three water-deficit (near-zero deficit or full irrigation, supplemental, and high deficit or dryland) regimes, replicated four times (total 60 plots). Water deficit conditions and insect infestations impacted crop growth profile as well as lint yield. For example, fleahopper infestation resulted in increased apical growth of the plants in water-deficit conditions, whereas sequential infestation of two insect pests increased the plant apical growth in irrigated plots (2018). Lint yield was similar across all five treatment combinations under dryland condition (2018 and 2019) while sequential infestations of two pests significantly reduced lint yield under dryland in 2020; the sequential infestation of two pests (2018) and cotton fleahopper augmentation (2019) significantly reduced the lint yield compared to untreated control under irrigated condition, indicating the impact of drought conditions on modulating the effect of insect pests as well as the plant's compensatory ability.

Economic Evaluation of Insect-Pest Management in Water-Deficit Cotton Production

INTRODUCTION

The Texas High Plains (THP) is a semi-arid region with characteristic low rainfall (average annual rainfall of 15-18 in.), with production agriculture supported by limited irrigation or rain-fed. As a result, the cropping system in this region is largely low-input and the producer decision-making in economically profitable input use is a challenge. THP has been facing some significant drought conditions in recent years, including the drought of 2011 that claimed much of the Texas production agriculture, reducing total cotton yield that year by 55%. Drought conditions ensued the next 3 years that disproportionately depleted the underground water, significantly shifting the cotton production outlook in THP to even more low input with dryland acreage reaching to about 70%. The shift in cotton production system due to devastating droughts in an already semi-arid region has altered our input resources, cultivars, and management practices. Low cotton market price, increased nitrogen fertilizer price, and reduced water availability have forced farmers to move toward reorganizing available input resources to sustain their production enterprise. While the drought and heat conditions are unpredictable, the anticipated changes in global climate patterns may exacerbate the water-deficit conditions further in the THP. Thus, transitioning to the new crop production reality via developing economic data-based input management practices has become our priority to sustain producer profitability and for future success of the U.S. cotton industry.

Much has been reported on direct and indirect effects of drought stress on cotton, but the effect of drought stress on cotton insect pest dynamics, feeding potential, and plant's response to insect injury under drought-stressed conditions are limited. In addition, the paucity of information on integration of pest management decisions and crop production decisions has hindered producers' ability to predict economic risks of optimizing limiting input resources. Predicting pest populations under different water-deficit crop production scenarios and understanding how these conditions influence those populations to impact crop production risks, are critically important components for implementing pest management strategies as crop cultivars and other input variables continue to change. Reduced water availability, low rainfall, higher pumping cost of limited water, and increased input cost may result in lower yields and correspondingly lower profit margins, warranting for higher water use efficiency in our crop production. Therefore, cotton producers must carefully consider costs of pest management options against potential benefits to overall net profit margin of the crop production enterprise. The objectives of this project are to: 1) Quantify the impact of five combinations of single versus sequential infestations of two major insects (thrips and cotton fleahoppers) on cotton lint yield and fiber quality under two irrigation water regimes (water-deficit treatments – near dryland versus full irrigation), and 2) Develop a dynamic optimization economic model that maximizes the net returns from management of single versus sequential pest infestations under water-deficit crop production conditions. Thus, the goal of this project aims to integrate production practices and pest management options under numerous cotton management scenarios (10 total scenarios) and the management options will be developed based on breakeven value and net return of each option for farmers to choose depending on the availability of water resource on their farms.

METHODOLOGY

A multi-year study was initiated in 2018 on a five-acre subsurface drip irrigation cotton field located at the Texas A&M AgriLife Research farm (Lubbock County, TX).

Irrigation water level treatments. Three irrigation water levels (dryland, supplemental irrigation, and full irrigation) simulated three water-deficit production conditions, including high water-deficit (dryland condition), limited water condition, and no water deficit. A high-water treatment maintained >90% evapotranspiration replenishment through subsurface drip irrigation throughout the crop growing season, supplemental irrigation maintained about 40% ET replenishment, and the dryland treatment received pre-planting irrigation to facilitate proper seed germination and no additional irrigation. In 2018, only dryland and full irrigation main plot treatments were available; 2019 and 2020 had three water levels.

Planting and field management. The 2018 study followed the conventional tillage system of cotton cultivation and regionally adopted production practices were followed, including pre-planting application of 80 lb N/acre. Cotton cultivar DP 1646 B2XF (seed with no insecticide or fungicide seed treatment) was planted on 31 May 2018. In 2019, wheat was planted on 14 February 2019 as a cover crop to minimize pre-planting soil erosion and prevent cotton seedlings from sandblasting during May/June. Cotton cultivar DP 1646 B2XF was planted on 14 May 2019 and the wheat was terminated on 20 May 2019 with Roundup WEATHERMAX® (48.8% glyphosate) @ 32 oz./Acre to facilitate thrips movement to emerging cotton seedlings. Other field management activities included the tank-mixed application of herbicide XTENDIMAX® (48.8% dicamba) @ 22 oz./Acre and Roundup WEATHERMAX® (48.8% glyphosate) @ 32 oz./Acre on 17 June 2019 for weed management, field cultivation on 24 June 2019 for soil aeration and weed management, and fertilizer application (100 lb. N/acre) via side-dressing on 23 July 2019. In 2020, cotton cultivar DP1820B3XF was planted on 18 May 2020 following pre-plant fertilizer application @ 80 lb N/Acre. Weed management was achieved via Roundup WEATHERMAX® (48.8% glyphosate) @ 32 oz./Acre and XTENDIMAX® (48.8% dicamba) @ 22 oz./Acre tank-mix applications on 18 May 2020 and 3 June 2020 and field cultivation on 21 July 2020 for soil aeration and weed management.

Insect infestation treatments. Two key insect-pest species (thrips and cotton fleahoppers) impacting cotton production risks were evaluated with five combinations of single versus sequential infestations under three water-deficit (zero, medium, and high) regimes, replicated four times (total 60 plots); only zero and high water-deficit regimes were evaluated in the 2018 study. Five possible insect infestation scenarios were evaluated where the infestations were simulated during the most vulnerable stage of cotton for each target insect (Table 1). Targeted insect management options were achieved via natural colonization and/or artificial augmentation of insect pests. Because THP cropping conditions rarely warrant more than a single insecticide application to suppress either of the two major insect pest groups (thrips at seedling stage and cotton fleahoppers at early squaring stage), this study was designed to infest the treatments at the most vulnerable stage of crop for the species infested.

Table 1. Five insect management scenarios evaluated under three irrigation water treatments, Lubbock, Texas, 2018-2019

Treatment #	Insect Infestation Treatment Simulated via Artificial Infestation
1	All insects suppressed (No insect infestation) (sprayed control)
2	Thrips occurring at 1-2 true leaf stage
3	Cotton fleahoppers occurring during the first week of squaring
4	Thrips and cotton fleahoppers infested sequentially
5	No insect management (untreated control)

2018 study

Thrips. Thrips were released to seedling cotton on 19 June 2018 when the crop was at 1-2 true leaf stage. Thrips infested alfalfa terminals were excised from a healthy alfalfa patch and these terminals were laid at the base of young cotton seedlings. Thrips were expected to move onto the cotton seedlings as excised alfalfa sections began to dry. Approximately 6 thrips per seedling were released to two 5 row-ft sections (approximately 12 plants per section) per plot (approximately 140 thrips per thrips-augmented plot). Thrips were released on all 16 thrips-augmentation plots (treatments #2 and #4 x 2 water levels x 4 replications) on the same day. Thrips were released on four additional plots to estimate thrips movement onto the cotton seedling via absolute sampling of seedlings and washing of thrips 3 days post-release. Data showed that the seedlings received an average of 1.2 live thrips per seedling which is the threshold density for 1-2 leaf stage seedling cotton.

Uncharacteristic high daytime temperatures for the next 7 days following the thrips release (103-107 ^{o}F) contributed to low thrips feeding performance and perhaps high thrips mortality after the thrips moved to the seedlings. Consequently, no visible signs of thrips-feeding effect were observed in thrips-augmented plots.

Cotton fleahoppers. Woolly croton, with embedded overwintering fleahopper eggs, was harvested from rangeland sites near College Station, Texas, in early February 2018 and then placed into cold storage. Eighty 1-gallon sheet metal cans, each containing 4 ounces of dry croton twigs per can, were initiated to generate the required number of cotton fleahopper nymphs for the experiment. Conditions conducive to cotton fleahopper emergence were simulated in a laboratory environment in order to induce hatching of overwintered eggs embedded in the croton stems, and emerged cotton fleahoppers were subsequently reared on fresh green beans. The single release of nymphal cotton fleahoppers (2nd instars) was timed to simulate the acute heavy infestation of cotton fleahoppers (4-5 days of feeding) while cotton was highly vulnerable to the fleahopper injury (1st week of squaring). The release was accomplished on 10 July 2018 by transferring second-instar fleahoppers from the laboratory colony into 15 cm X 10 cm plastic containers, then cautiously depositing them onto the terminals of plants in each treatment plot at the rate of 5 nymphs per plant. Immediately after cotton fleahoppers were released onto the fleahopper-augmentation plots (treatments #3 and #4; total 16 plots), control plots were sprayed with Orthene® 97. All treatment

plots, except treatment #1, were sprayed with Orthene® 97 on 17 July 2018 and kept insect-free for the remainder of the study to isolate the effect of various treatments.

The flowering profile was monitored from all 40 experimental plots for five sample dates (31 July, 6 August, 9 August, 15 August, and 28 August 2018) to determine the effect of insect infestation and water-deficit condition on fruiting delays and/or flowering patterns. Plant height was also recorded from all plots at the time of harvest. Hand harvesting was done on 16 November 2018 from flagged area and cotton was ginned on 17 December 2018. Lint samples were analyzed at Cotton Incorporated for fiber parameters.

2019 study

Thrips. Wheat cover was terminated on 20 May 2019 with glyphosate to facilitate thrips movement to emerging cotton seedlings to achieve natural infestation of thrips on experimental plots. Uncharacteristic heavy rain events during 23-26 May (4.51" rainfall) with associated small hail event compromised the study field for desired plant stand. Thrips were all dislodged from the wheat cover as well as those already transferred to cotton seedlings. Therefore, thrips were manually augmented on two 5-ft sections per treatment plots on 4 June 2019 via collecting immature thrips from nearby alfalfa terminals and releasing them onto the cotton seedlings, by placing thrips-infested alfalfa terminals at the base of each seedling @ approximately 5 thrips per cotton seedling. This rate of infestation is expected to result in about 1 thrips per seedling after 80% mortality of released thrips. Unexpected storms occurred on 5 and 6 May with additional 1" of rain dislodging all released thrips. We re-released thrips on 7 June 2019, but the ensuing hot and windy days following the second release did not allow thrips to colonize in the experimental plots. Consequently, we assumed no thrips effect on our experimental plots. Nevertheless, we conducted the visual ranking of the experimental plots on 11, 17, and 22 June 2019 to discern if any thrips-induced injury was inflicted on the seedlings. We found no thrips-inflicted injury nor observed any thrips colonization.

Cotton fleahoppers. Woolly croton, with embedded overwintering fleahopper eggs, was harvested from rangeland sites near College Station, Texas, 18 February 2019 and then placed into cold storage. Eighty 1-gallon sheet metal cans, each containing 4 ounces of dry croton twigs per can, were initiated on 10 May 2019 to generate the required number of cotton fleahopper nymphs for the study. Conditions conducive to cotton fleahopper emergence were simulated in a laboratory environment in order to induce hatching of overwintered eggs embedded in the croton stems, and emerged cotton fleahoppers were subsequently reared on fresh green beans. Cotton fleahopper emergence began on 19 June 2019. The single release of nymphal cotton fleahoppers (2^{nd} instars) was timed to simulate the acute heavy infestation of cotton fleahoppers (4-5 days of feeding) while cotton was highly vulnerable to the fleahopper injury (1^{st} week of squaring). The release was accomplished on 4 July 2019 by transferring second instar fleahopper nymphs from the laboratory colony onto the terminals of plants in each treatment plot at the rate of 5 nymphs per plant. Control plots had no insect activity to warrant any insecticide intervention. Unfortunately, a heavy rainfall occurred on 6 July 2019 (2.75") and dislodged the released cotton fleahoppers and the treatment deployment was totally ineffective. The field was too wet to re-augment the cotton fleahopper within the next 2-3 days, but another storm passed through west Texas on 11 July 2019 that brought a damaging hail onto our field, causing significant damage to the test plots. Consequently, the crop stand was very poor with significant hail damage to the growing terminals for the crop to perform normally. Nevertheless, we introduced a manual square-removal treatment to selected control plots

to evaluate the simulated fleahopper-induced square removal and resulting crop growth profile across three irrigation treatments. However, the unusual rainfall patterns might have already compromised our irrigation treatments. Treatments #1 and #3 were sprayed with BRACKET® 97 (acephate 97%) @ 3 oz./acre on 7 and 17 June 2019 to ensure insect-free plots to isolate the effect of insect-release plots. Square removal treatment was deployed on 26 July 2019 by removing 100% squares from all plants in two 5-row ft sections per plot. Plant mapping was conducted 10 days after cotton fleahopper release to assess the fruit set on all experimental plots.

We also monitored flowering profile by counting number of white flowers in two 5-row ft sections per experimental plots twice a week (23, 26, and 30 July, 2, 5, 9, 12, 16, 19, 23, 26, and 30 August, and 3 and 11 September) during the cotton flowering period (total 14 sample dates). Pre-harvest plant mapping was done on 30 October 2019 and hand harvesting was done on 1 November 2019 from flagged area. Cotton was ginned on 14 November 2019 and the lint samples were sent to Cotton Incorporated for fiber analysis.

2020 study

Thrips. Thrips sampling was performed via whole-plant removal of 10 seedlings per plant in a mason jar for later processing of the samples in the laboratory to extract thrips from plant washing technique. Thrips samplings were done on 29 May, 1 June, 4 June, and 11 June 2020. Treatments #1 and #3 were sprayed with BRACKET® 97 (acephate 97%) @ 3 oz./acre on 29 May and 8 June to ensure insect-free plots to isolate the effect of thrips. Because natural thrips colonization was insignificant, thrips were manually augmented on two 6-ft sections per treatment plots on 20 June 2020 via collecting immature thrips from nearby alfalfa terminals and releasing them onto the cotton seedlings, by placing thrips-infested alfalfa terminals at the base of each seedling @ approximately 10 thrips per cotton seedling. This rate of infestation was expected to result in about 2 thrips per seedling after 80% mortality of released thrips. Thrips-released plots were visually inspected three times to assess for thrips colonization. We found no apparent thrips-inflicted injury on these test plots.

Cotton fleahoppers. Woolly croton, with embedded overwintering fleahopper eggs, was harvested from rangeland sites near College Station, Texas, 2 February 2020 and then placed into cold storage. Forty 1-gallon sheet metal cans, each containing 4 ounces of dry croton twigs per can, were initiated on 15 June 2020 to generate the required number of cotton fleahopper nymphs for the study. Conditions conducive to cotton fleahopper emergence were simulated in a laboratory environment in order to induce hatching of overwintered eggs embedded in the croton stems, and emerged cotton fleahoppers were subsequently reared on fresh green beans. Cotton fleahopper emergence began on 24 June 2020. The single release of nymphal cotton fleahoppers (2^{nd} instars) was timed to simulate the acute heavy infestation of cotton fleahoppers (4-5 days of feeding) while cotton was highly vulnerable to the fleahopper injury (1^{st} week of squaring). The release was accomplished on 2 July by transferring second-instar fleahoppers from the laboratory colony onto the terminals of plants in each treatment plot at the rate of 5 nymphs per plant. Control plots had no insect activity to warrant any insecticide intervention. Unfortunately, a heavy windstorm occurred in the evening of 2 July and likely compromised the fleahopper colonization in the plant. In addition, we introduced a manual square-removal treatment to selected plots to evaluate the crop growth profile across three irrigation treatments. Plant mapping was performed on July 28 to assess the cotton fleahopper-induced injury.

Temporal flower pattern was monitored for 14 sampling dates, starting on 20 July and conducted every 2-3-day intervals. Harvest aids Boll'd® 6SL (Ethephon [(2-chloroethyl) phosphonic acid] @ 1 qt//A (boll opener) and Folex® 6 EC (S, S, S-Tributyl phosphorotrithioate) 1 pint/A (defoliant) were applied on 12 October to accelerate opening of matured unopened bolls and begin the defoliation process. Test plots were hand-harvested on 23 October. Hand-harvested yield samples were ginned, and fiber analysis was performed at Cotton Incorporated for HVI parameters.

RESULTS

2018 study

Extremely high temperatures during the seedling stage complicated the study in 2018, especially the released thrips failed to exert the desired significant infestation on the young cotton seedlings. As a result, thrips damage to seedlings was not apparent on visual observation. Cotton fleahoppers caused about 20% square loss overall across all experimental plots. Because cotton fleahoppers were released when plants had 2-3 total squares (all were fleahopper susceptible squares), the effect was not apparent immediately and plants outgrew the effect of early season fleahopper-induced square loss. Nevertheless, insect injury manifested some noticeable effect on flowering patterns, plant height, and lint yield.

Untreated control plots showed slightly higher flower densities in irrigated versus dryland cotton effect all throughout the month-long monitoring period, with significantly higher flower densities in late August. Contrasting to this phenomenon, the flowering patterns were near identical between irrigated and dryland plots when cotton fleahoppers were infested singly or sequentially with thrips infestation (Fig. 1). When thrips were infested alone, flowering patterns between dryland and irrigated main-plot treatments were generally similar to what was observed in untreated or sprayed control plots. Overall, average flower abundance was similar across five insect augmentation treatments within each irrigation treatment (Fig. 2). While cotton flowering occurs daily during the active flowering period and the average of flower monitoring only five times may not reflect the production potential of cotton, these patterns clearly indicate that insect infestation, particularly cotton fleahoppers, rendered overall flowering patterns between irrigated and dryland similarly (Figs. 1-2). The average flower abundance was significantly lower in dryland compared to that in irrigated cotton only at untreated control plots while all other treatments were not significantly different between the two irrigation regimes (Fig. 2). These data suggest that the insect infestation during pre-flower stage exerts some significant physiological response to cotton during the flowering stage. Multi-year data will hopefully add more insights into this phenomenon.

Pre-harvest plant measurement showed that insect-augmented plots in irrigated cotton had significantly taller plants compared to that in untreated control plots, but the effect was considerably diminished under dryland conditions (Fig. 3). There was significant "noise" on plant height data under dryland condition in which fleahopper-infested plants resulted in the tallest plants while thrips followed by fleahoppers resulted in the shortest plant heights. We find no reasonable explanation for why cotton fleahopper-infested plots resulted in both tallest and shortest plants.

Lint yield was significantly higher in irrigated cotton compared to that in dryland cotton across all five treatment combinations (Fig. 4). This suggests that the dryland plots were sufficiently water-stressed during the growing season, despite several rainfall events during the crop maturation

phase in late September - early October. The highest lint yield under irrigation treatment was observed in the untreated control treatment (1,607 lb/acre), while the lowest (1,253 lb/acre) was recorded in the thrips+fleahopper sequential infestation treatment (Fig. 4). Lint yield in other treatments (spray control, thrips only, and fleahoppers only) did significantly differ from the untreated control or thrips+fleahopper sequential treatments (Fig. 4). Lint yield did not significantly vary across five insect augmentation treatments. As expected, the yield threshold in dryland cotton was much lower than that for irrigated cotton and thus the lower yield across all treatments can be partially attributed for lack of insect treatment effect on lint yield.

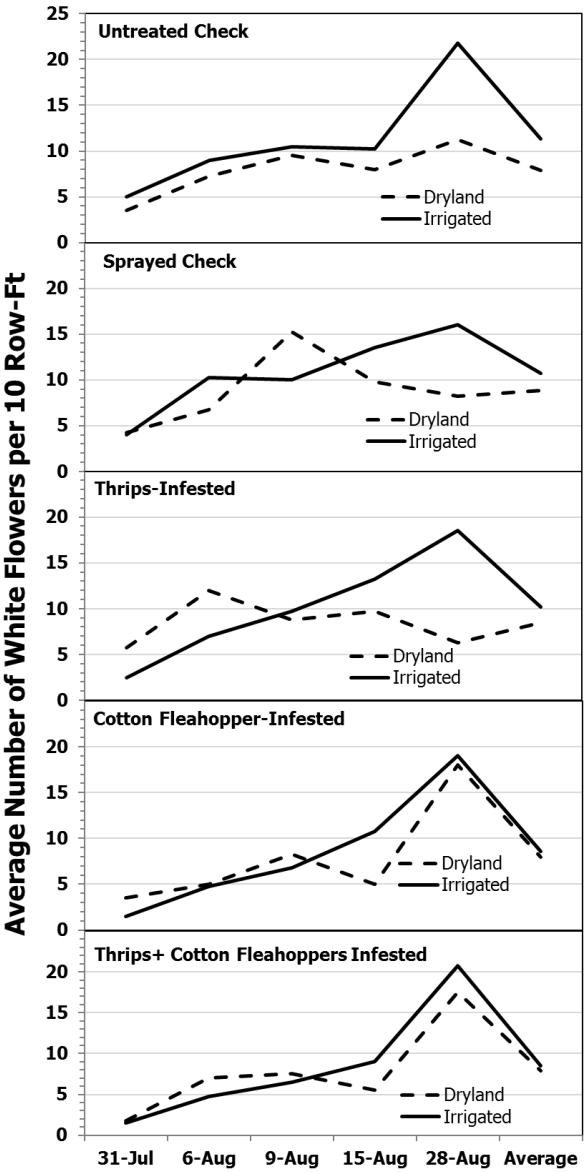

Figure 1. Temporal abundance of white flowers (number of white flowers per 10 row-ft per sample date) recorded from thrips and fleahopper infested plots under dryland versus irrigated production conditions, Lubbock, Texas, 2018.

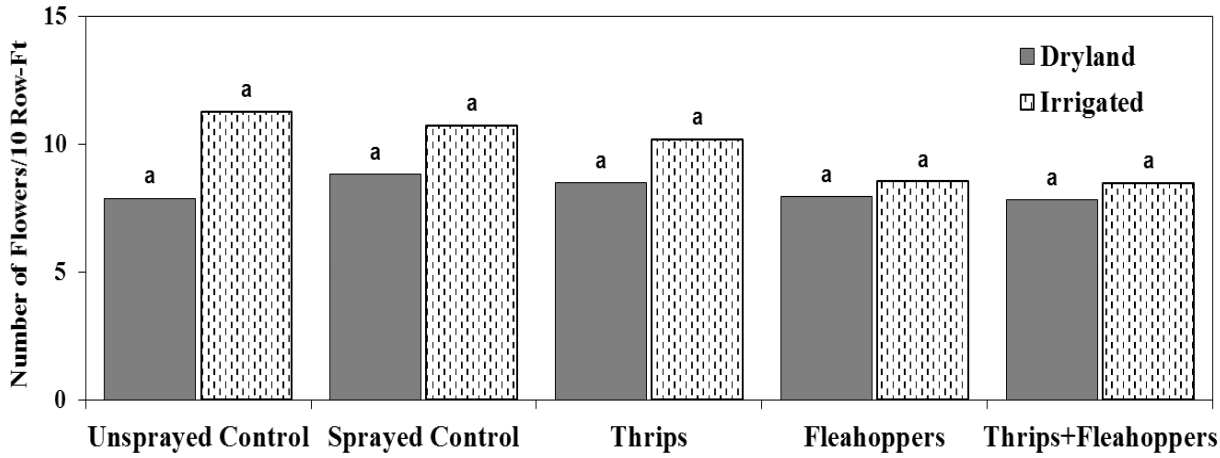

Figure 2. Average abundance of white flowers (number of white flowers per 10 row-ft; n=5 sample dates) recorded from thrips and fleahopper infested plots under dryland versus irrigated production conditions, Lubbock, Texas, 2018. Average values were compared across five treatments within each irrigation treatment; same lowercase letters indicate treatment means were not significantly different from each other.

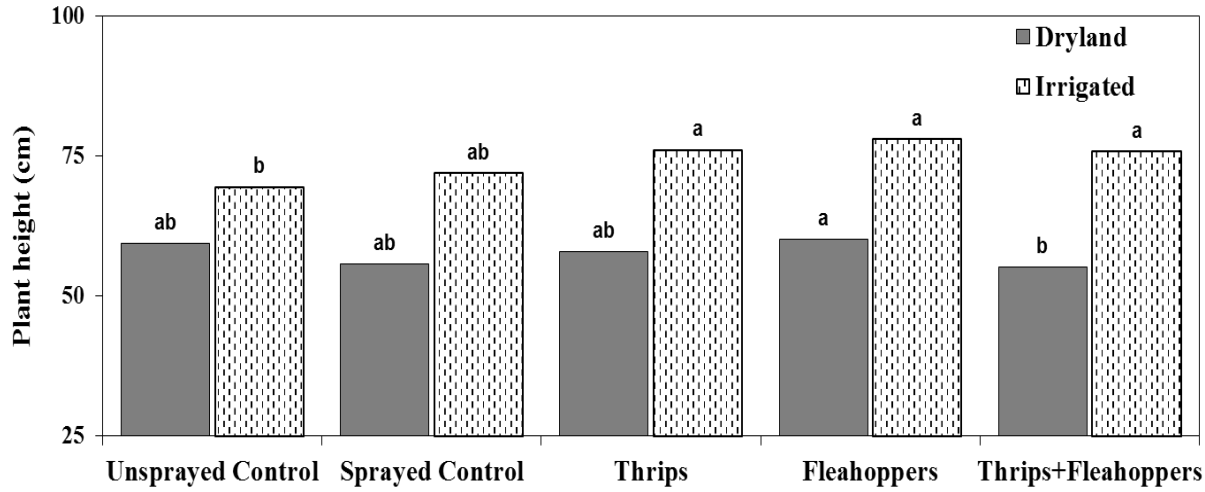

Figure 3. Plant height impacted by thrips and fleahopper infestations under dryland versus irrigated production conditions, Lubbock, Texas, 2018. Average values were compared across five treatments within each irrigation treatment; same lowercase letters indicate treatment means were not significantly different from each other.

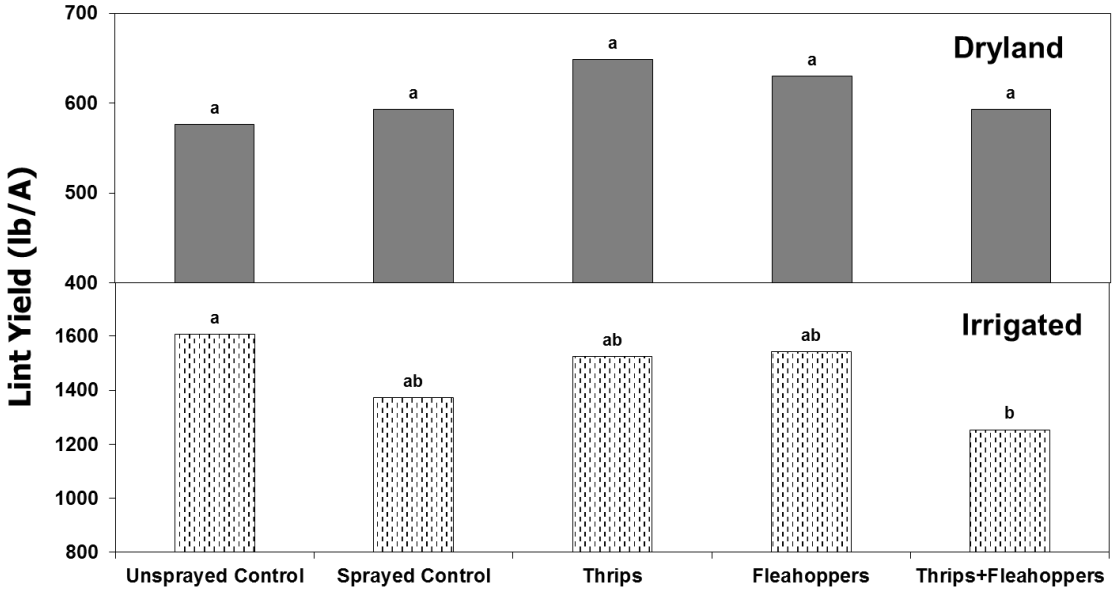

Figure 4. Cotton lint yield losses due to thrips and fleahopper infestation under dryland versus irrigated production conditions, Lubbock, Texas, 2018. Average values were compared across five treatments within each irrigation treatment; same lowercase letters indicate treatment means were not significantly different from each other.

2019 study

Atypical heavy rain events during the pre-squaring stage of cotton with associated small hail event compromised the early season portion of the study. Thrips were all dislodged from the wheat cover as well as those already transferred to cotton seedlings. Manually augmented thrips also suffered from recurring storm events and thrips could not colonize in the study plots. As stated in the Methods section above, we effectively abandoned the possibility of exerting thrips-induced injury effect on seedling cotton. Visual ranking of the experimental plots indicated no evidence of thrips-inflicted injury nor we observed any thrips colonization.

Cotton fleahopper augmentation resulted in 50-55% square abortion compared to 15-20% abortion in control plots; square abortion was similar between dryland and full irrigation plots (Fig. 5). While significant weather events occurred soon after cotton fleahoppers were released, the fleahopper augmentation exerted significant square loss as desired.

Untreated control plots and sprayed control plots showed higher flower densities in both irrigated and dryland cottons compared with that in insect augmented plots; this difference was more pronounced in irrigated plots than in dryland plots (Fig. 6). Full irrigation and supplemental irrigation plots displayed similar flowering patterns throughout the season. The plots with manual square removal to mimic cotton fleahopper-induced square loss displayed synchronized fruiting patterns across irrigation treatments. Overall, average flower abundance was similar amongst unsprayed control, sprayed control, and manual square removal plots, whereas the flower abundance on these three treatments were generally higher than that in all other insect augmented treatments; this trend was similar across all three irrigation water levels (Fig. 6). These patterns clearly indicate that insect infestation, particularly cotton fleahoppers, rendered overall flowering patterns between irrigated and dryland similarly. The average flower abundance was significantly

lower in dryland compared to that in irrigated cotton at control plots while other treatments were not consistent across water treatments. These data suggest that the insect infestation during pre-flower stage exerts some significant physiological response to cotton during the flowering stage.

Pre-harvest plant measurement showed that insect augmentation treatments did not result in increased plant heights as observed in 2018. It was expected because the early rain/hailstorm events had severely thinned out the plant stand which allowed plants to grow laterally rather than adding the mainstem nodes following insect infestations. Nevertheless, plots in irrigated cotton had significantly taller plants compared to that in dryland plots as expected.

Lint yield was significantly higher in irrigated cotton (both full and supplemental) compared to that in dryland cotton across all five treatment combinations (Fig. 7). This suggests that the dryland plots were sufficiently water-stressed during the growing season, despite several rainfall events during the early to mid-season; there was a noticeable drought condition during the latter part of the growing season. The highest lint yield under full irrigation treatment was observed in the untreated control treatment (1,268 lb/acre), while the lowest (883 lb/acre) was recorded in the fleahopper infestation treatment (Fig. 7). These were the only treatments that resulted in significant yield difference. Lint yield did not significantly vary across insect augmentation treatments. Under dryland condition, lint yield did not significantly vary across treatments. As expected, the yield threshold in dryland cotton was much lower than that for irrigated cotton and thus the lower yield across all treatments can be partially attributed for lack of insect augmentation treatment effect on lint yield. Also, lint yield was generally similar between supplemental and full irrigation main treatments, owing to frequent rainfall events during early and mid-season that provided sufficient moisture profile in root zones in supplemental irrigation plots to carry the crop's water demand through the season. Thrips only treatment resulted in significantly lower yield under supplemental irrigation compared to that in other treatments (Fig. 8). However, we are unable to speculate the reason for this yield reduction since there were no visible thrips injury during the early growth period of the crop.

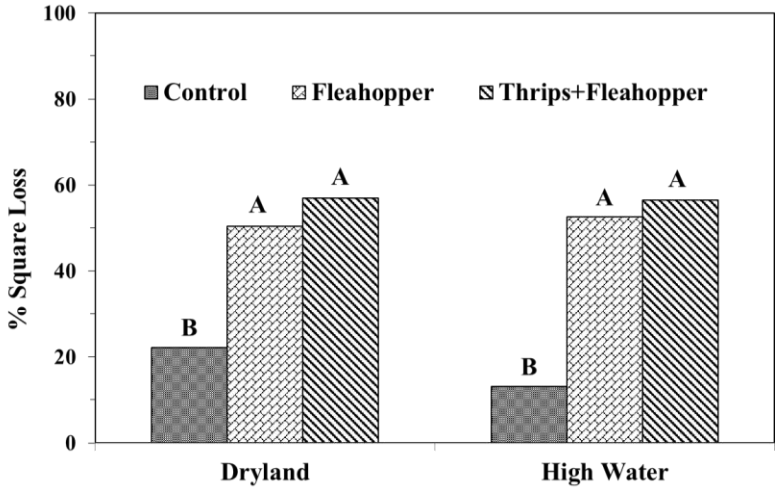

Figure 5. Percentage square loss (number of missing squares with respect to total squares set per plant) recorded following cotton fleahopper infestations in dryland versus full irrigation production conditions, Lubbock, Texas, 2019.

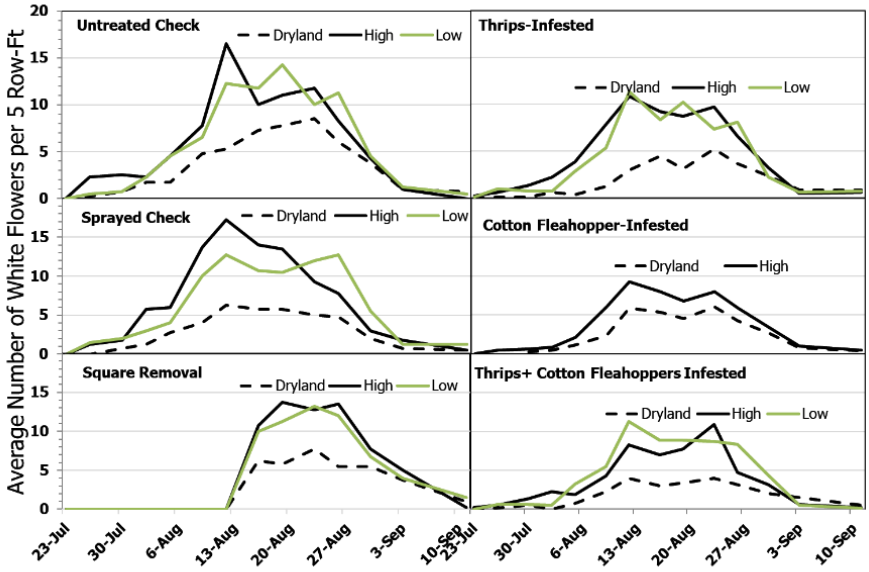

Figure 6. Temporal abundance of white flowers (number of white flowers per 5 row-ft per sample date) recorded from insect-release treatment plots under dryland, supplemental (low), and full (high) irrigation production conditions, Lubbock, Texas, 2019.

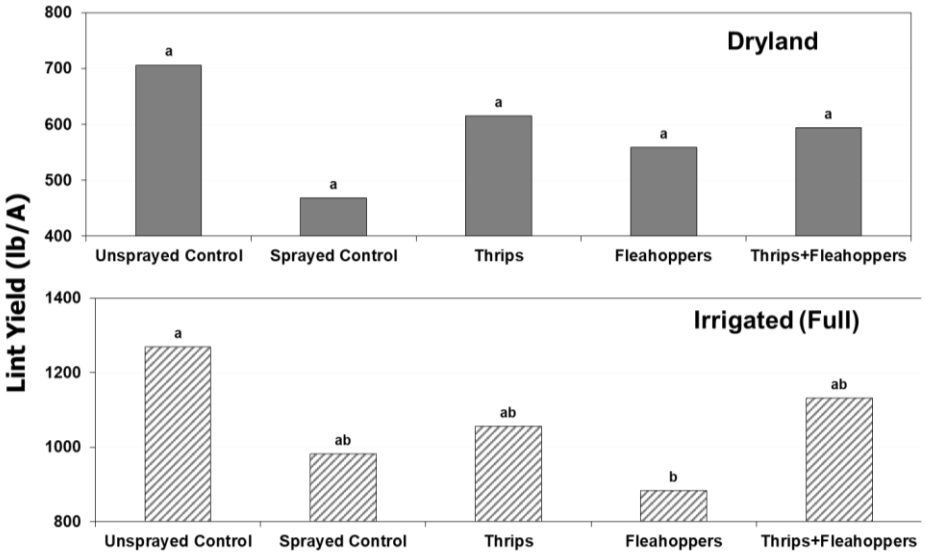

Figure 7. Cotton lint yield losses due to thrips and fleahopper infestations under dryland versus full irrigation production conditions, Lubbock, Texas, 2019. Average values were compared across five treatments within each irrigation treatment; same lowercase letters indicate treatment means were not significantly different from each other.

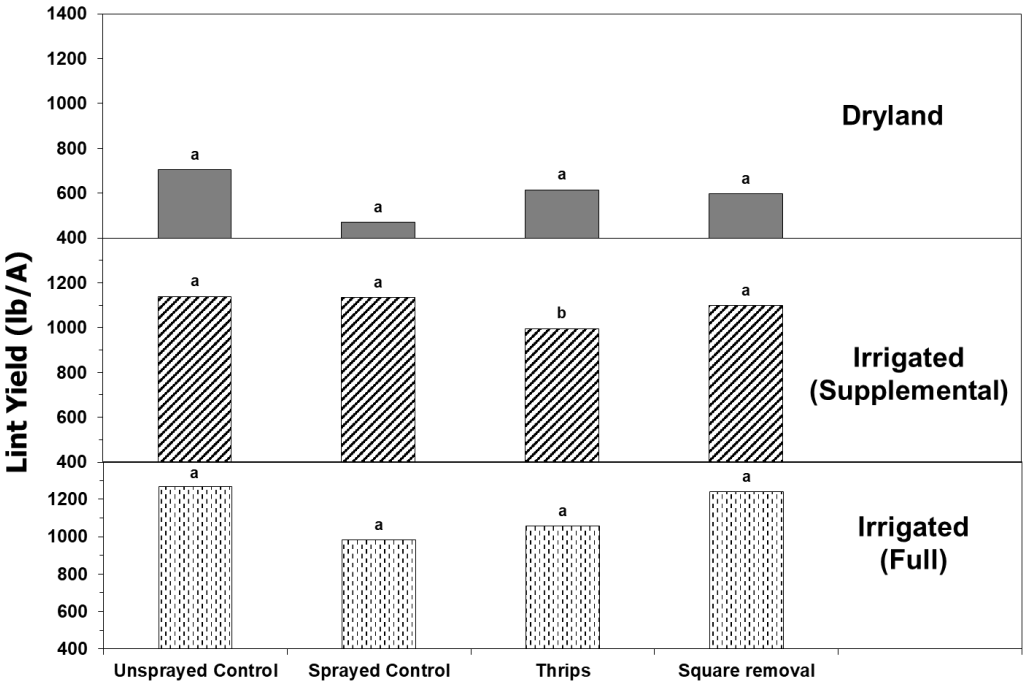

Figure 8. Cotton lint yield losses due to thrips and manual square removal (100% squares pruned at first flower stage to mimic severe cotton fleahopper damage) under three irrigation water regimes, Lubbock, Texas, 2019. Average values were compared across four treatments within each irrigation treatment; same lowercase letters indicate treatment means were not significantly different from each other.

2020 study

The natural thrips colonization was also insignificant in 2020 as in previous two years. Because natural colonization was inconsequential, thrips were manually augmented per treatment plots. Nevertheless, environmental conditions (e.g., incessant dry wind) did not allow thrips to colonize and exert significant injury to the plants in test plots. Therefore, the manual augmentation did very little to exert injury pressure on cotton plants. Similarly, a heavy windstorm occurred in the evening of 2 July and likely compromised the fleahopper colonization in the plant. As a result, cotton fleahoppers exerted mild injury pressure on plants, which caused about 10-14% square abscission and only increased plant height and more nodes on mainstem compared to that in control plots. The plant height effect, too, was only evident under dryland conditions as the irrigated plots all compensated this low level of early fruit abscission.

Because fleahopper-induced square loss was not significant, flowering profile was generally similar across all treatments. Nevertheless, considerable variations existed amongst treatments on temporal flowering patterns. Uninfested and sprayed control plots showed greater flower densities earlier than cotton fleahopper and thrips+cotton fleahopper infested plots (Fig. 9). Clearly, insect infested plots delayed peak flowering and even had slightly fewer total flowers than the uninfested plots. Limited irrigation plots showed greater flower densities in most treatments, but insect-infested treatments had conspicuously lower flower densities for limited irrigation plots during the early reproductive phase of the crop compared to that for uninfested plots (Fig. 9, left versus right

panel). High irrigation plots had the lowest flower densities compared to low irrigation or dryland plots under thrips+fleahopper infested treatment. The plots with manual square removal to mimic cotton fleahopper-induced square loss displayed similar fruiting patterns across irrigation treatments. Even at low rate of insect-induced square removal during pre-flower stage, significant physiological responses can be exerted to cotton during the flowering stage.

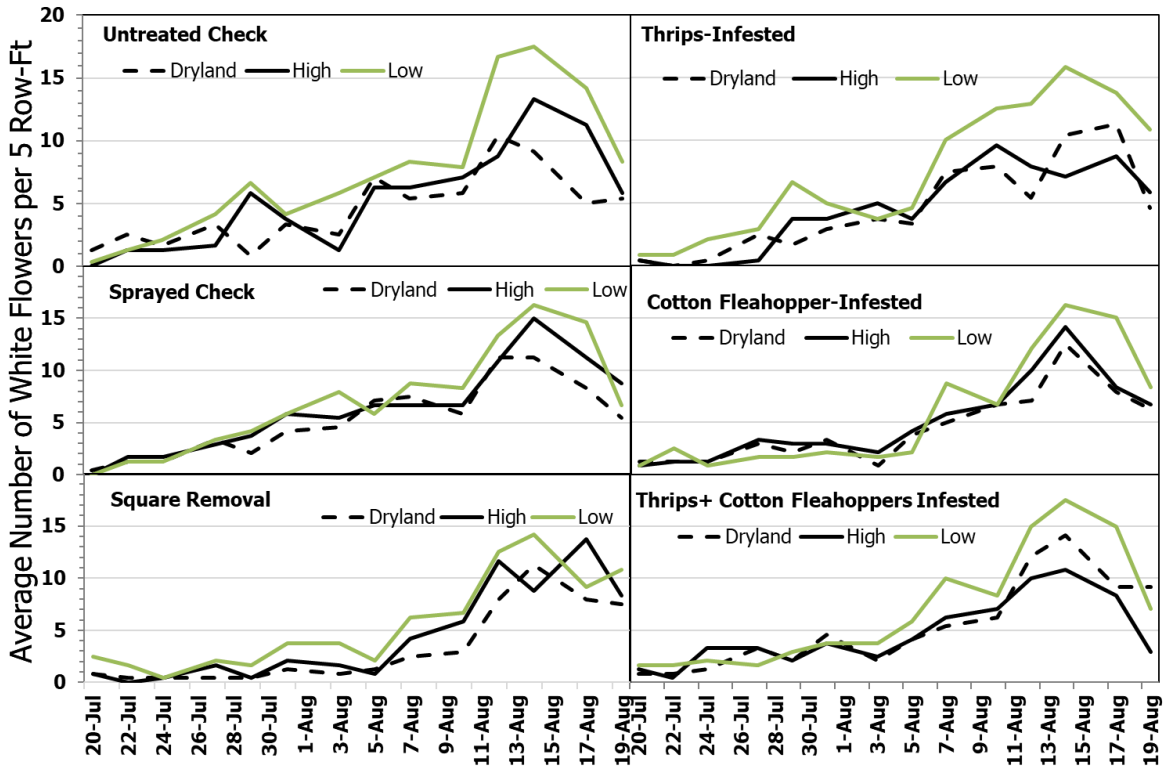

Figure 9. Temporal abundance of white flowers (number of white flowers per 5 row-ft per sample date) recorded from insect-release treatment plots under dryland, supplemental (low), and full (high) irrigation production conditions, Lubbock, Texas, 2020.

As expected, lint yield varied with irrigation treatments. Lint yield was significantly higher in irrigated cotton (High irrigation: 1623 lb/acre; Low irrigation: 1350 lb/acre) compared to that in dryland (1046 lb/acre) cotton across all five treatment combinations (Fig. 10). This suggests that the dryland plots were sufficiently water-stressed during the growing season. The highest lint yield under full irrigation treatment was observed in the uninfested control treatment (1877 lb/acre), while the lowest (890 lb/acre) were recorded in the thrips and thrips+fleahopper infestation treatments (Fig. 10). Overall, thrips+fleahopper treatment resulted in the lowest yield across all three irrigation treatments, although statistically significant only under dryland condition. Another conspicuous trend was that fleahopper alone treatment that exerted only 10-14% square loss did not significantly rendered the yield loss. It is known from the past studies that a low level of fleahopper injury compensates or even overcompensates the insect-induced fruit loss. However, when fleahopper caused even a low-level injury sequentially with a low-level thrips injury, yields were reduced considerably across all irrigation treatments. The lack of statistical significance across sub-treatments under irrigated treatments can be attributed to a large variation in data.

Although thrips infestation and thrips-induced injuries were insignificant, lint yields were numerically (irrigated plots) or significantly (dryland) lower across all irrigation treatments.

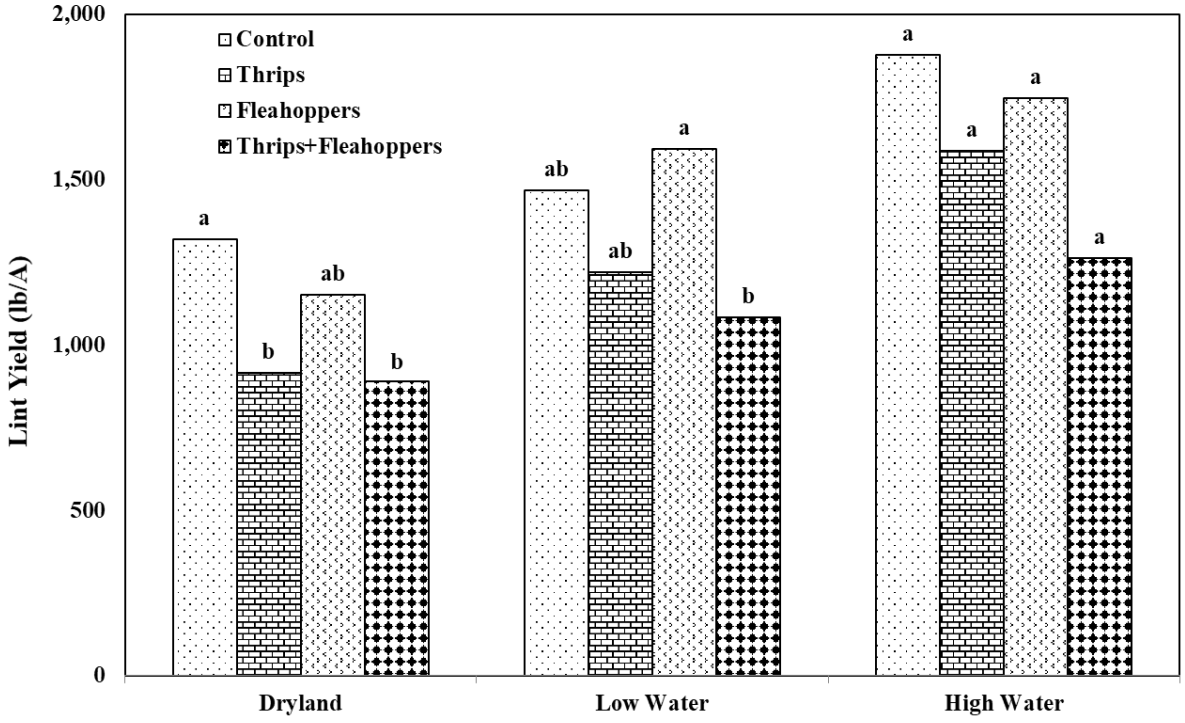

Figure 10. Cotton lint yield losses due to thrips and fleahopper infestations under three irrigation water treatments, Lubbock, Texas, 2020. Average values were compared across four treatments within each irrigation treatment; same lowercase letters indicate treatment means were not significantly different from each other.

Overall, irrigation treatments did not significantly alter the HVI parameters. However, there was a considerable irrigation x insect infestation interaction in influencing the fiber parameters (Fig. 11). In general, low level of thrips and fleahopper injuries appeared to increase micronaire values, except for low irrigation. In fact, uninfested control plots had the micronaire in the discount range under both dryland and high irrigation treatments, whereas all insect-infested plots had micronaire in premium range (high irrigation) or premium/base range (dryland). It was interesting to note that the micronaire values were at base range for low irrigation treatment for all insect-augmentation treatments. Other fiber parameters, including fiber length, uniformity, strength, and elongation were generally similar across all insect-infestation treatments within each irrigation level (Table 2). Irrigation water treatment had only marginal effect on other HVI parameters.

Table 2. HVI fiber quality parameters influenced by thrips and cotton fleahopper infestation singly as well as sequential infestation of both insects under three irrigation water treatments, Lubbock, Texas, 2020

Fiber Parameters	Irrigation Treatment	Uninfested Control	Thrips	Fleahopper	Thrips+ Fleahopper
Micronaire	Dryland	3.40	4.39	4.51	4.24
Fiber length	Dryland	1.13	1.14	1.16	1.14
Uniformity	Dryland	80.43	80.88	81.60	80.90
Strength	Dryland	31.80	31.35	32.35	31.13
Elongation	Dryland	7.68	7.68	7.83	7.70
Micronaire	Low	3.83	4.42	4.30	4.30
Fiber length	Low	1.16	1.15	1.16	1.15
Uniformity	Low	81.66	82.05	81.63	81.90
Strength	Low	31.60	31.63	32.00	31.75
Elongation	Low	7.99	7.90	7.93	7.93
Micronaire	High	3.39	3.96	4.24	4.16
Fiber length	High	1.17	1.20	1.21	1.19
Uniformity	High	80.94	81.35	82.23	82.28
Strength	High	31.71	31.55	31.78	32.03
Elongation	High	8.11	8.15	8.30	8.15

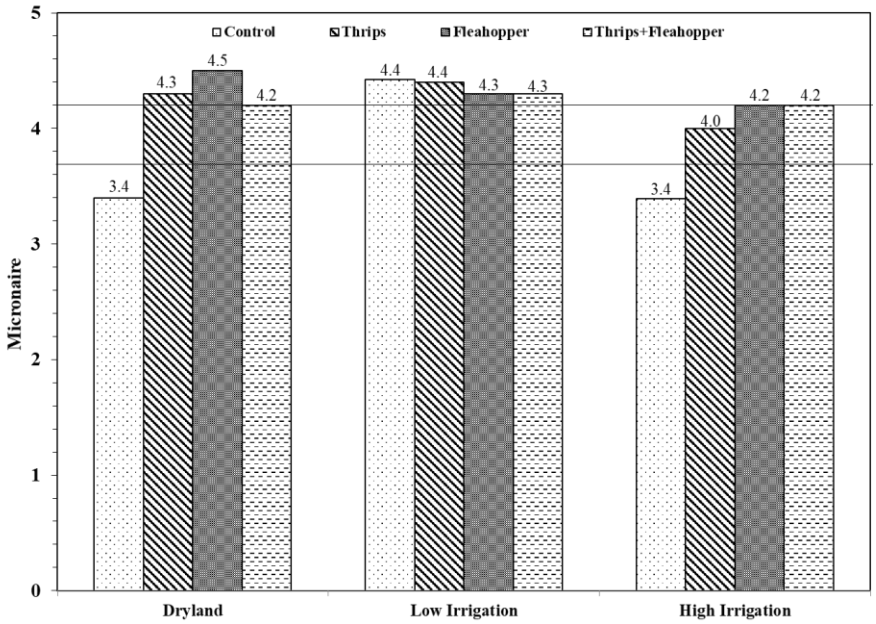

Figure 11. Cotton fiber micronaire (units) values influenced by thrips and fleahopper infestations under three irrigation water treatments, Lubbock, Texas, 2020. Average values between 3.7-4.2 indicate premium cotton fiber.

We plan to develop the structure of the profitability model using these three years of data prior to planting the 2021 crop. These data will be used to analyze and compare the economics of management of thrips and cotton fleahoppers singly or in sequential combinations under three water-deficit production regimes. A set of economic profitability models will empower cotton producers in production decision-making in their specific production scenarios (insect pest management options in relation to water availability in their production enterprises). Economic decision-making models will be developed based on crop yield response and crop budget analyses. Crop yield response functions will be generated for each of the 5 insect management treatments within each water-deficit production systems, with 10 separate production scenarios. Cotton yield response to each insect treatment under three water levels will be fitted to calculate the slope (coefficient) of each treatment. Functional form will consider cotton yield and insect exposure (treatment) as fixed effect, and year as random. Insect management treatments within each water level will be ranked based on likelihood ratio test. Although the last three years of data were highly variable and inconsistent between the years, we expect that these data will help us develop the foundation of the model and the final year of data will aid in refining the management model.

Acknowledgments

Research funding which facilitated this study came from Cotton Incorporated Texas State Support Committee. Dol Dhakal provided the technical help.

IMPACT OF *LYGUS* BUGS ON COTTON FIBER YIELD AND QUALITY UNDER SUPPLEMENTAL AND FULL IRRIGATION PRODUCTION CONDITIONS

Dol P. Dhakal
Abdul Hakeem
Megha N. Parajulee
Katie L. Lewis
Texas A&M AgriLife Research and Extension Center
Lubbock, Texas

Abstract

The impact of late season *Lygus* infestation on cotton yield and fiber quality was assessed under supplemental and high irrigation regimes. Two cotton varieties and two *Lygus* densities were evaluated using field cages. Cages were removed a week after release of bugs and plants were sprayed with an insecticide to achieve an acute infestation. In another study, 20% bolls were removed from the top third of the plant to mimic late season *Lygus* infestation. The study revealed that the impact of *Lygus* injury was more pronounced under water-deficit growing conditions; likely because late-season lint yield compensations were limited due to reduced water availability limiting continued boll growth and fiber development. *Lygus* bugs significantly reduced lint yield both in supplemental and full irrigated cotton; however, cotton in water-deficit condition was more severely impacted by *Lygus* than under fully irrigated cotton. Cotton variety DP 1823NRB2XF performed better both in supplemental irrigation and full irrigation treatments than DP 1830B3XF.

Introduction

Lygus appears to be an increasing concern for the Texas High Plains growers in recent years. *Lygus* bugs utilize >300 host species including cotton in the cotton growing regions of the United States. The shift in cotton production system from 60:40% irrigated:dryland to 40:60% in the last decade has altered the cotton production practices. This shift from irrigated to dryland farming warranted to manage cotton pests effectively to increase profitability. Plant bugs have a general inclination to attack the stressed plants and cause significant damage. Cotton plant responses to *Lygus* injury under a range of irrigation regimes remain uninvestigated. The overall goal of this study was to characterize the effects of drought conditions on *Lygus* infestation behavior and plant response to *Lygus* injury.

Materials and Methods

A multi-year study was conducted in a multi-factor split-plot randomized block design with two water levels (full irrigation vs supplemental irrigation) and two infestation levels (*Lygus* augmented versus control). In 2018, *Lygus* were collected from nearby alfalfa fields and released in cages. *Lygus* were released on one 3-ft cotton row section per plot. Multi-plant (5-7 plants) cages were used to contain the released insects. The control plots were flagged and sprayed with insecticides. One plant from each treatment was removed and processed for *Lygus* damage assessment. Number of fruits aborted and internal/external boll damage as well as number of damaged seeds per boll were recorded. In 2019, a 5-ft section was flagged, and 20% bolls were removed from the top third of the plant to mimic *Lygus* bug infestation. Plants within flagged area were harvested, and lint yield and quality were determined.

Results and Discussion

Lygus bugs significantly reduced lint yield both in supplemental and full irrigated cottons; however, cotton in water-deficit condition was more severely impacted by *Lygus* than under fully irrigated cotton. DP1820B3XF had numerically lower lint yield than DP1823NRB2XF in both supplemental and full irrigation treatments (Fig. 1). In cotton variety DP1820B3XF, percent yield reduction was 48% in supplemental irrigation while percent yield reduction in full irrigation was 31%; however, in DP 1823NRB2XF, percent yield reduction in supplemental irrigation was 23% while the reduction in full irrigation was 21%. Thus, DP1823NRB2XF performed better both in supplemental and full irrigation treatments in our production situation (Fig. 2). In 2019, significantly higher lint yield was recorded from control plots in full (high) water treatments than simulated treatments. No differences in lint yield was recorded amongst treatments in low (supplemental) water treatments (Fig. 3).

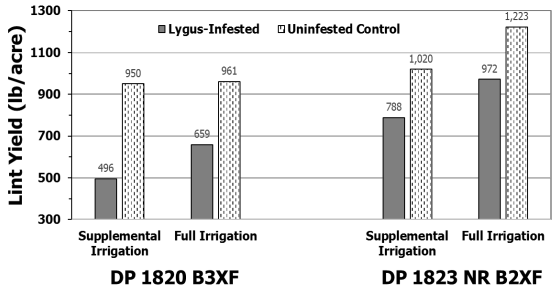

Figure 1. Cotton lint yield losses due to *Lygus* infestation under supplemental versus full irrigation production conditions, Lubbock, Texas, 2018.

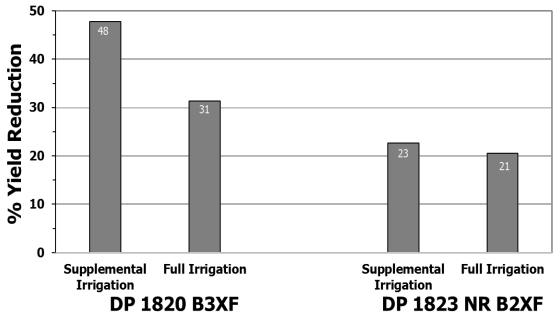

Figure 2. Percent lint yield losses in two cotton cultivars due to *Lygus* infestation under supplemental versus full irrigation production conditions, Lubbock, Texas, 2018.

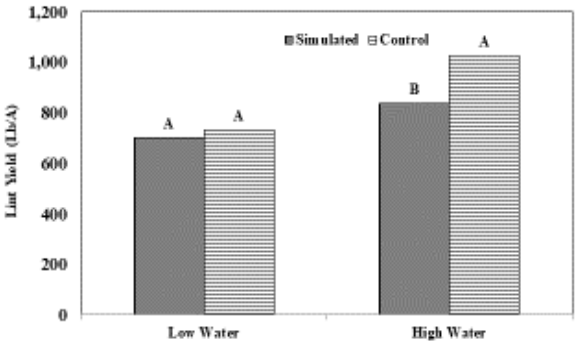

Figure 3. Cotton lint yield losses observed due to *Lygus* simulated damage under supplemental vs full irrigation, Lubbock, Texas, 2019.

References

Parajulee, M., A. Hakeem, and K. Lewis. 2018. Impact of *Lygus* bugs and cotton fleahoppers on cotton yield under drought conditions. Proceedings, Beltwide Cotton Conferences, National Cotton Council, Memphis, TN.

Hakeem, A., J. Jordan, Parajulee, M., E. Backus, and F. Cervantes. 2018. Effect of carbon nanotubes on feeding behavior of *Lygus hesperus* (Hemiptera: Miridae) in cotton: An electropenetrographic evaluation. Proceedings, Beltwide Cotton Conferences, National Cotton Council, Memphis, TN.

Shrestha, R., S. Carroll, W. McSpadden, M. Parajulee. 2012. Overview of *Lygus* research and outreach program in the Texas High Plains: Serving the clientele of the world's largest cotton patch. The 3rd International *Lygus* Symposium, Scottsdale, Arizona.

MANAGING EARLY-SEASON INSECT PESTS IN DRYLAND COTTON

Abdul Hakeem
Megha Parajulee
Texas A&M AgriLife Research and Extension Center
Lubbock, TX
Michael Toews
University of Georgia, Department of Entomology
CAES Campus
Tifton, GA
Suhas Vyavhare
Katie Lewis
Donna McCallister
Dol Dhakal
Texas A&M AgriLife Research and Extension Center
Lubbock, TX

Abstract

A multi-year study has been initiated in the Texas High Plains to quantify the impact of single (thrips or cotton fleahoppers) versus multiple (thrips and cotton fleahoppers sequentially) pest infestations on cotton lint yield and fiber quality under two irrigation water regimes. The scope of this work entails integrating production practices and pest management options under numerous cotton management scenarios. Thrips and cotton fleahoppers were evaluated with five combinations of single versus sequential infestations under two water-deficit (near-zero deficit or full irrigation and high deficit or dryland) regimes, replicated four times. Thrips and cotton fleahopper augmentations and resulting colonization were compromised due to uncharacteristic rain and storm events. Plant growth parameters such as plant height, leaf area and dry leaf biomass were significantly higher in full irrigation plots than dryland plots. Water deficit conditions and insect infestations impacted crop growth profile as well as lint yield. Lint yield was similar across all five treatment combinations under dryland conditions while cotton fleahopper significantly reduced the lint yield compared to control under high irrigated condition.

Introduction

The Texas High Plains (THP) has been facing some significant unpredictable drought conditions in recent years. THP is a semi-arid region with characteristic low rainfall, with production agriculture supported by limited irrigation or rain-fed. As a result, the cropping system in this region is largely low-input and the producer decision-making in economically profitable input use is a challenge. Since 2007, water-deficit cotton production situation has worsened in THP and dryland:irrigated cotton production has shifted from 40:60 to 60:40 in recent years. Unpredictability of limited rainfall has been a challenge for cotton farmers in their production decision-making. Increased input costs and decreased availability of water have forced growers to move toward reorganizing available input resources to sustain their production enterprise.

Drought has direct and indirect effects on cotton, but the information on the effect of drought stress on cotton insect pest dynamics, feeding potential, and plant's response to insect injury under drought-stressed conditions are limited. Predicting pest populations under water-deficit cropping production scenarios and understanding how these conditions influence those populations to impact crop production risks are critically important components for implementing pest management strategies as crop cultivars and other input variables continue to change. The objective of this study was to quantify the impact of early-season pests on cotton lint yield and fiber quality under dryland and high irrigation water regimes.

Materials and Methods

Irrigation water level treatments

Two irrigation water levels (dryland and full irrigation) were evaluated in this study. A high-water treatment maintained >90% evapotranspiration replenishment through subsurface drip irrigation throughout the crop growing season whereas the dryland treatment received pre-planting irrigation to facilitate proper seed germination and no

additional irrigation. Cotton cultivar DP 1646B2XF (seed with no insecticide or fungicide seed treatment) was planted on 14 May 2019.

Insect infestation treatments

Two key early-season insect-pest species (thrips and cotton fleahoppers) impacting cotton production risks were evaluated with five combinations of single versus sequential infestations under two water-deficit (zero versus high) regimes, including sprayed control and unsprayed control, replicated four times (total 40 experimental plots). Targeted insect management options were achieved via artificial infestation of insect pests as our experiment was designed to infest our treatments at the most vulnerable stage of crop for the species infested.

Insect augmentation

Thrips. Thrips were released to seedling cotton on 7 June 2019 when the crop was at 1-2 true leaf stage. Thrips infested alfalfa terminals were excised from a healthy alfalfa patch and these terminals were laid at the base of young cotton seedlings. Thrips were expected to move onto the cotton seedlings as excised alfalfa sections began to dry. Approximately 6 thrips per seedling were released to two 5 row-ft sections (approximately 12 plants per section) per plot (approximately 140 thrips per thrips-augmented plot), with 20% expected survivorship of released thrips.

Cotton fleahoppers. Woolly croton, with embedded overwintering cotton fleahopper eggs, was harvested from rangeland sites near College Station, Texas, in early February 2019 and then placed into cold storage. Eighty 1-gallon sheet metal cans, each containing 4 oz of dry croton twigs per can, were initiated to generate the required number of cotton fleahopper nymphs for the experiment. Conditions conducive to cotton fleahopper emergence were simulated in a laboratory environment in order to induce hatching of overwintered eggs embedded in the croton stems, and emerged cotton fleahopper nymphs were subsequently reared on fresh green beans. The single release of nymphal cotton fleahoppers (2^{nd} instars) was timed to simulate the acute heavy infestation of cotton fleahoppers (4-5 days of feeding) while cotton was highly vulnerable to the fleahopper injury (1^{st} week of squaring). The release was accomplished on 4 July by transferring second-instar fleahopper nymphs from the laboratory colony into 15 cm x 10 cm plastic containers, then cautiously depositing them onto the terminals of plants in each treatment plot at the rate of 5 nymphs per plant. Immediately after cotton fleahoppers were released onto the fleahopper-augmentation plots, control plots were sprayed with Orthene® 97.

Parameters measured

The flowering profile was monitored from all 40 experimental plots for eight sample dates to determine the effect of insect infestation and water-deficit condition on fruiting delays and/or flowering patterns. Five plants from each plot were removed to record plant height, leaf area, and dry leaf biomass. Hand harvesting was done on 4 November 2019 from flagged area and cotton was ginned on 12 November 2019. Lint samples were sent to Cotton Incorporated for fiber analysis.

Results and Discussion

No significant differences were observed in thrips numbers between control-spray treatments and thrips-released treatments due to recurring storm events preventing thrips from effectively colonizing on the cotton seedlings. Plant parameters such as plant height, leaf area, and dry leaf biomass were significantly influenced by the irrigation water level, with greater plant height, larger leaf, and greater biomass in full irrigation plots compared to that in dryland plots (Figs. 1-2). As expected, lint yield was significantly higher in full irrigation treatments than dryland treatments. No significant differences in lint yield was observed amongst treatments in dryland plots; however, in irrigated plots, significantly higher lint yield was recorded from unsprayed control plots compared to that in fleahopper augmented plots (Fig. 3).

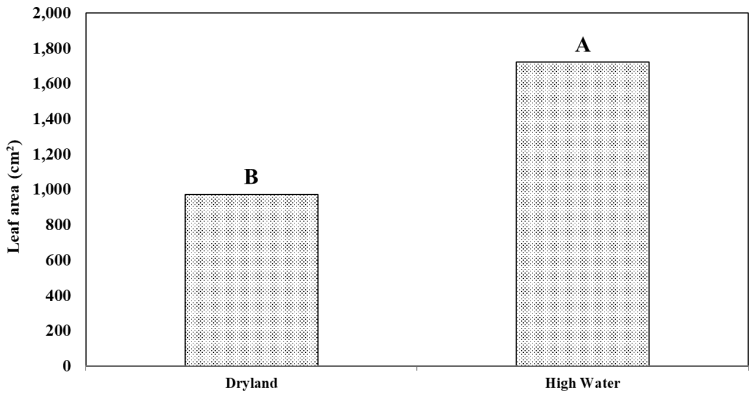

Figure 1. Leaf area recorded from dryland and high irrigation treatment plots, Lubbock, Texas, 2019. Different letters indicate treatment means were significantly different from each other.

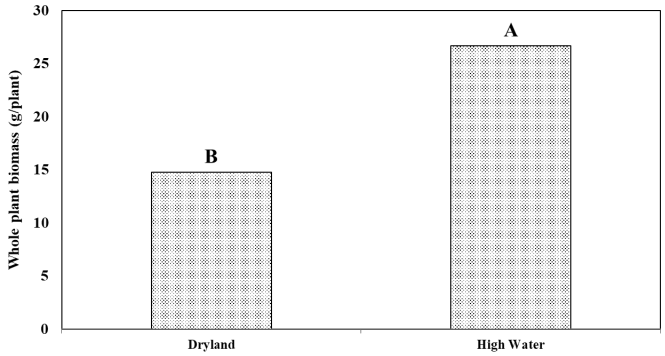

Figure 2. Plant dry biomass (peak-flowering stage) recorded from dryland and irrigation treatment plots, Lubbock, Texas, 2019. Different letters indicate treatment means were significantly different from each other.

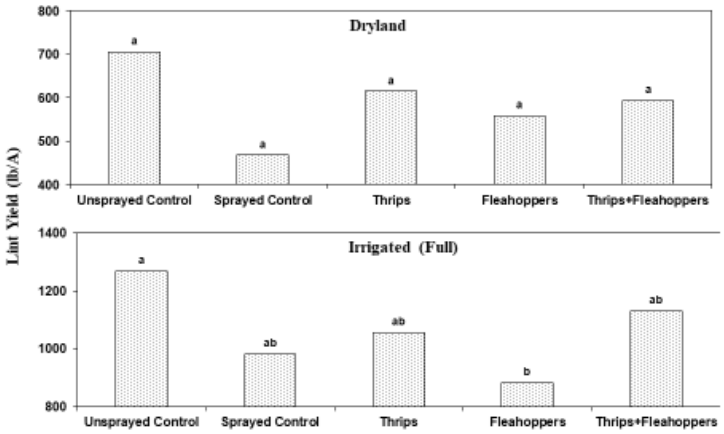

Figure 3. Cotton lint yield losses due to thrips and cotton fleahopper infestations under dryland versus irrigated production conditions, Lubbock, Texas, 2019. Average values were compared across five treatments within irrigation main treatment; same lowercase letters indicate treatment means were not significantly different from each other.

As noted previously, the 2019 crop season in the Texas High Plains was marked with uncharacteristic rain and thunderstorms which compromised our irrigation treatments. There was no evidence of thrips colonization nor any thrips-induced injury in our experimental plots. Cotton fleahoppers were also dislodged by heavy storms and probably did not cause injury to the growing squares as expected, but the plant mapping 10 days after cotton fleahopper release

indicated significant square loss in fleahopper augmented plots. While no significant treatment differences were observed under dryland regime, cotton fleahopper augmented plots resulted in lowest yield under irrigated system. However, the yield was highly variable across treatments; thus, the results of the 2019 study are inconclusive. This study will be repeated for three additional years.

Acknowledgements

This study was supported by Cotton Incorporated Texas State Support Committee and Plains Cotton Improvement Program.

References

Parajulee, M. N., R. B. Shrestha, and J. F. Leser. 2006. Influence of tillage, planting date, and Bt cultivar on seasonal abundance and within-plant distribution patterns of thrips and cotton fleahoppers in cotton. International Journal of Pest Management 52: 249-260.

Rummel, D. R., and M. D. Arnold. 1989. Estimating thrips populations in cotton with conventional sampling and a plant washing technique. Southwestern Entomologist 14: 279-285.

EFFECT OF NITROGEN FERTILITY RATES ON COTTON CROP RESPONSE TO COTTON FLEAHOPPER DAMAGE

Megha N. Parajulee
Dol P. Dhakal
Abdul Hakeem
Ziyan NanGong
Katie L. Lewis
James P. Bordovsky
Texas A&M AgriLife Research
Lubbock, TX

Abstract

A long-term field study was conducted to examine the effect of soil nitrogen (residual nitrogen plus applied nitrogen) on cotton agronomic growth parameters and cotton compensation following cotton fleahopper induced fruit loss under a drip irrigation production system. Fixed-rate nitrogen application experimental plots, previously established and fixed for 12 years prior to the initiation of this study in 2014, consisted of five augmented nitrogen fertility levels (0, 50, 100, 150, and 200 lb/acre) with five replications. Each year, soil in each experimental plot was sampled for residual nitrogen analysis prior to planting. Rates of applied N exceeding 100 lb/acre resulted in 40-80 lb/acre residual nitrogen detection during the following season. Cotton fleahopper-induced fruit loss was generally compensated at low N as well as at high N, whereas optimum N was the most vulnerable to fleahopper-induced injury. Simulated fruit loss was generally compensated across all N application rates.

Introduction

Nitrogen fertility limits cotton production yields in the Texas High Plains. A Texas High Plains study under a limited irrigation production system (Bronson et al. 2006) characterized the effect of nitrogen application on leaf moisture and leaf nitrogen content in cotton and the resulting influence on cotton aphid population dynamics (Matis et al. 2008). Leaf nitrogen content did not vary with nitrogen application method (variable N versus blanket N application of an optimal amount), but both the blanket application and variable-rate application resulted in significantly higher leaf nitrogen contents than were noted in zero-augmented nitrogen plots. As nitrogen application rates were increased from zero to an optimum rate, a significant decrease in both aphid birth and death rates occurred, translating to a decrease in crowding and an increase in aphid survival (Matis et al. 2008). While these data help to characterize cotton aphid population dynamics between zero nitrogen fertility management and optimal nitrogen application rates, the population dynamics of cotton aphids and other cotton arthropods have not been examined under a full range of nitrogen fertility rates (Parajulee et al. 2006, 2008). In particular, no known study has produced plant growth parameters or fruiting profile data pertaining to a spectrum of nitrogen application rates in cotton. The objective of this study was to evaluate, in cotton growing under a subsurface drip irrigation production system, cotton crop growth parameters and cotton's ability to compensate for cotton fleahopper induced fruit loss as influenced by varying N fertilizer application rates.

Materials and Methods

The study was conducted at the Texas A&M AgriLife Research farm near Plainview, Texas. A 5-acre sub-surface drip irrigation system had been in place for 12 years prior to this study. Plot-specific nitrogen fertility treatments had been applied in a randomized block design with five replications since 2002. Five nitrogen application rates (0, 50, 100, 150, 200 lb/acre) had been deployed to the same experimental units consistently for 12 consecutive years to induce maximum discrimination among treatment plots through variation in soil residual nitrogen.

The study reported herein was conducted for six years (2014-2019). Soil residual nitrogen was monitored annually by taking two 24-inch core samples from each plot. The 0-12-inch portions of each core were combined to form a single, composite soil sample, and likewise, the 12-24-inch portions were combined, resulting in two samples per experimental plot. Samples were sent to Ward Laboratories, Kearny, Nebraska for analysis. Regionally well-adapted cultivars were used in this study over the duration of the study: FM 9063B2F was planted on 19 May 2014, FM 9180B2F on 18 May 2015, FM 1900GLT on 27 May 2016 and 4 May 2017, and NG3406 B2XF on 25 May 2018 and 4 June 2019. The experiment consisted of a randomized block design with five treatments and five replications. The

five treatments included side-dress applications of nitrogen fertilizer at rates of 0, 50, 100, 150, and 200 lb N/acre. Cotton was planted (56,000 seeds/acre) in 30-inch rows and was irrigated with a subsurface drip irrigation system.

Soil samples were taken from the experimental plots on 10 July (2014), 26 June (2015), 1 July (2016), 20 June (2017), 22 June (2018), and 26 June (2019) for residual nitrogen analysis. Crop growth and insect activity were monitored throughout the season. Fertility treatments were applied on 23 July (2014), 21 July (2015), 8 July (2016), 3 July (2017), 3 July (2018), and 19 July (2019) with a soil applicator ground rig. In 2014-2015, each plot received two cotton fleahopper treatments (5 adults per plant vs. no fleahopper as control), contained in multi-plant cages, within designated row sections two weeks into cotton squaring, the most critical phenological stage of cotton for fleahopper management in the Texas High Plains, to simulate an acute infestation of cotton fleahoppers. In 2016-2019, 100% squares were removed from treatment plots at first flower to simulate the cotton fleahopper induced square loss versus control (only data from 2018 and 2019 are included in this paper). Crop growth and fruiting patterns were monitored during the crop season. Pre-harvest plant mapping was done, and hand-harvested yield samples were obtained from each plot. Fiber samples were analyzed for lint quality parameters at the Cotton Incorporated Fiber Testing Laboratory (North Carolina).

Results and Discussion

Averaged over the entire 17-year study, soil residual N levels were significantly higher in plots that received the three highest application rates of N fertilizer versus plots receiving 50 lb/acre N or no N augmentation (Fig. 1). The highest N augmentation plots (200 lb/acre) had significantly highest average residual N (84 lb/acre); the year-to-year residual N was always the highest amount in this treatment, at least numerically. The two second highest N augmentation plots (100 and 150 lb/acre) resulted in significantly higher amount of soil residual N compared to that in zero and 50 lb/acre plots.

As expected, lint yield varied with N level regardless of the cotton fleahopper infestation. In uninfested control plots, lint yield displayed a characteristic staircase effect of nitrogen rate, with lowest lint yield in zero N and highest lint yield in 200 N treatments, with numerical increase in lint yield for each incremental nitrogen application of 50 lb/acre. Combined over all N treatments, the acute infestation of cotton fleahoppers rendered the lint yield reduction from 975 and 910 lb/acre in the uninfested control to 846 and 877 lb/acre in fleahopper augmented treatments in 2014 and 2015, respectively. In both years, cotton lint yield was not significantly affected by ~25% fleahopper-induced square loss three weeks into squaring at both zero N and 200 lb/acre plots, either via insect-induced pruning of undesirable fruit load (zero N) or compensation (200 lb N), whereas lint yield was significantly lower in fleahopper augmented 50 to 100 lb/acre plots (only 100 lb/acre treatment in 2015) compared to that in uninfested plots (Fig. 2), clearly suggesting that the plant response to cotton fleahopper injury is greatly influenced by nitrogen fertility. At 100 lb/acre N, plants were unable to compensate the cotton fleahopper-induced yield loss consistently in both years of the study, which may likely be attributed to N limitation (Fig. 2). On the other hand, simulated damage mimicking cotton fleahopper severe infestation (100% square loss at first flower) through manual pruning was generally compensated regardless of the applied N rates, except that there was a marginal reduction in yield at highest N levels in 2018 (Fig. 3).

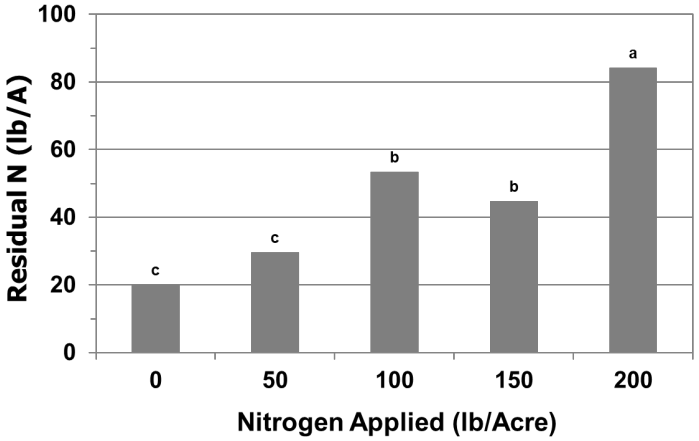

Figure 1. Average (2002-2019) yearly residual nitrogen as influenced by varying rates of applied nitrogen.

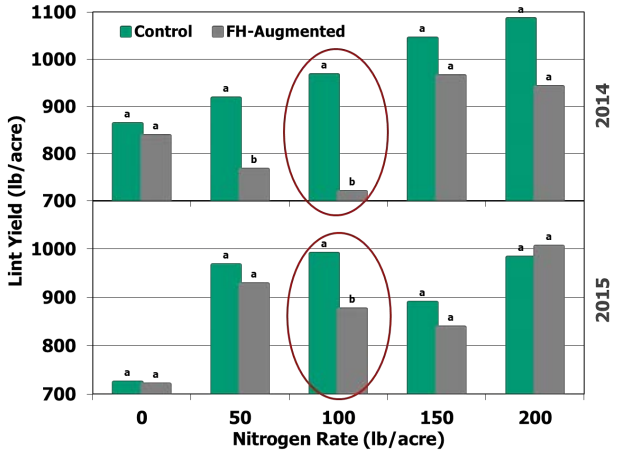

Figure 2. Effect of nitrogen augmentation rates on lint yield following a single acute infestation of cotton fleahopper versus uninfested control, 2014-2015.

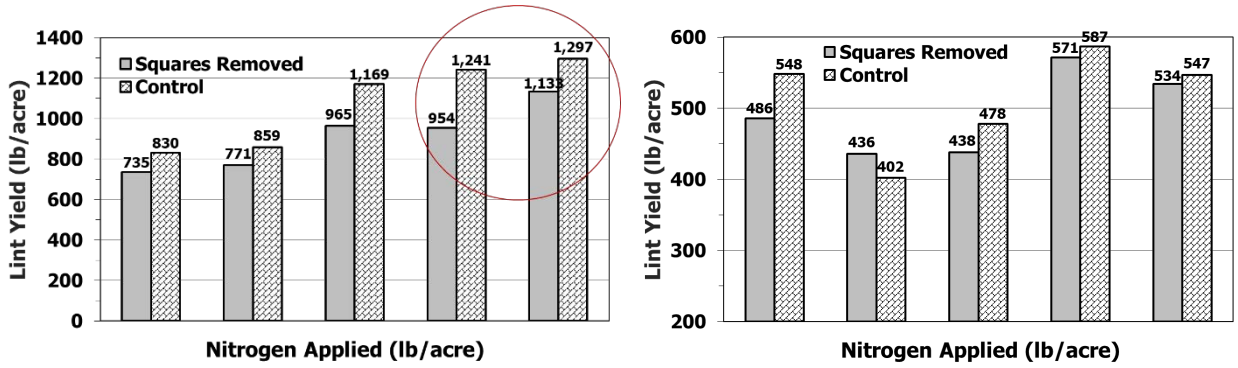

Figure 3. Effect of nitrogen augmentation rates on lint yield following a simulated severe infestation of cotton fleahopper versus uninfested control, 2018-2019.

Acknowledgments

Cotton Incorporated Core Program and Plains Cotton Growers, Inc. provided partial funding for this long-term nitrogen fertility study.

References

Bronson, K. F., J. D. Booker, J. P. Bordovsky, J. W. Keeling, T. A. Wheeler, R. K. Boman, M. N. Parajulee, E. Segarra, and R. L. Nichols. 2006. Site-specific irrigation and nitrogen management for cotton production in the Southern High Plains. *Agronomy Journal* 98: 212-219.

Matis, T. I., M. N. Parajulee, J. H. Matis, and R. B. Shrestha. 2008. A mechanistic model based analysis of cotton aphid population dynamics data. *Journal of Agriculture and Forestry Ecology* 10: 355-362.

Parajulee, M. N., R. B. Shrestha, and J. F. Leser. 2006. Influence of tillage, planting date, and *Bt* cultivar on seasonal abundance and within-plant distribution patterns of thrips and cotton fleahoppers in cotton. *International Journal of Pest Management* 52: 249-260.

Parajulee, M. N., R. B. Shrestha, A. K. Barman, and S. C. Carroll. 2008. Ecologically intensive pest management in cotton agroecosystems: *Lygus hesperus* as a model system. *Egyptian Journal of Agricultural Research* 86: 57-81.

HISTOPATHOLOGICAL EFFECTS OF A PROTEIN COMPLEX PURIFIED FROM XENORHABDUS NEMATOPHILA ON THE MIDGUT OF HELICOVERPA ARMIGERA LARVAE

Qin-Ying Wang
Shuqin Liu
Xiao-Xiao Guo
Zi-Yan NanGong
Plant Protection College, Hebei Agricultural University
Hebei, China
Meghan Parajulee
Texas A&M AgriLife Research and Extension Center
Lubbock, Texas, USA

Abstract

Entomopathogenic nematodes in the field carry symbiotic bacteria (Xenorhabdus or Photorhabdus) into the host insect through a natural orifice or the body wall and then release the symbiotic bacteria into the blood cavity of the insect. The symbiotic bacteria multiply and release a variety of active substances, including insecticidal proteins, which kill the host insect rapidly. In this study, a protein complex (named Xnpt) with insecticidal activity was isolated from X. nematophila HB310 strain using methods of salting out and native polyacrylamide gel electrophoresis (PAGE). Six polypeptides ranging 50~250 kDa were well separated from Xnpt protein by sodium dodecyl sulfate (SDS)-PAGE. Xnpt showed growth inhibition effect on the neonates of Helicoverpa armigera and destroyed the excised peritrophic membrane of H. armigera. The histopathology of Xnpt to H. armigera fourth-instar larvae was studied by dissecting and olefin slice of the midgut. The midgut tissues of the larvae began to change after treated with Xnpt (500 ng/mL) orally in 6 hours. The forepart of the peritrophic membrane began to fracture, and the midgut cells extended. The epithelium was decomposed gradually, and the midgut tissues were loose or disordered. The peritrophic membrane disappeared at 12 h but appeared again at 72 h following transient or sublethal exposure to the toxin. The histological analysis of H. armigera larvae midgut showed that Xnpt has extensive histopathological effects on the host tissues.

Introduction

Xenorhabdus spp. and Photorhabdus spp. are symbiotically associated with nematodes of the families, Steinernematidae and Heterorhabditidae, respectively. Entomopathogenic nematodes such as Steinernematidae and Heterorhabditidae carry symbiotic bacteria into the blood cavity of host insect and then release the symbiotic bacteria. The bacteria produce toxins to overcome immune response of insect hosts and kill their hosts. A family of oral and injectable insecticidal toxins produced by Xenorhabdus and Photorhabdus has been identified (Blackburn et al. 1998). Bowen et al. (1998) isolated several kinds of Tc from Photorhabdus luminescens W14 and reported that the histopathology of the Manduca sexta midgut following oral Tca treatment was very similar to that described for the δ-endotoxins from Bacillus thuriqiensis (Bowen et al. 1998). It implies that these bacteria have the potential to be developed as insecticidal agents. Xenorhabdus nematophila HB310 was isolated from Steinernema carpocapsae HB310. We isolated a toxin complex with oral activity from X. nematophila HB310 and described the influence of the toxin protein on the Helicoverpa armigera larvae.

Methods

H. armigera larvae and X. nematophila HB310 were obtained from the Pest Biocontrol Insectary, Hebei Agricultural University. Toxin complex was obtained using the methods such as salting out and native-PAGE from the cells of X. nematophila HB310 (Wang et al. 2005). H. armigera neonates and fourth-instar larvae were placed in the wells of a 24-well cell-culture plate filled with diet and held in an incubator at 26±1°C. The diet was either treated with phosphate (PBS) buffer as an untreated control, or with toxin complex (protein concentration 5.19 μg /g diet). Symptoms of toxicity were noted, and survivors were weighed 120 h after the initiation of the bioassay. Three replicates were used for each treatment, with 72 total insects per treatment.

Fourth-instar larvae of H. armigera were transferred to the artificial diet treated with 20 μL of toxin complex (51.9 μg/mL). The peritrophic membranes (PMs) were obtained by dissecting the treated larvae midguts at 6, 12, 24, 36, 48, 60, 72, and 96 h. The difference between control and treatment was observed at the same period of time. Ten insects were dissected per treatment.

The midguts from the fourth-instar larvae of H. armigera were dissected and immediately fixed in Bouin's fluid. The fixed larvaal midguts were then embedded in paraffin, and 5 μm sections were cut. The sections were stained with eosin and hematoxylin and mounted with glycerol for microscope imaging.

Results and Discussion

We isolated every protein band from the native-PAGE spectrum of X. nematophila HB310 intracellular protein extracts (Fig 1). Bioassay results indicated that the oral insecticidal activity of the second protein band was higher than that of other bands to H. armigera neonates. This protein was named as Xnpt complex (Fig.1). In the SDS-PAGE spectrum, this protein complex was separated to more bands. Xnpt complex showed strong growth inhibition effect on the neonates of H. armigera. After 5 days of feeding, the larva that fed toxin were considerably smaller compared to the larvae in control (Table 1).

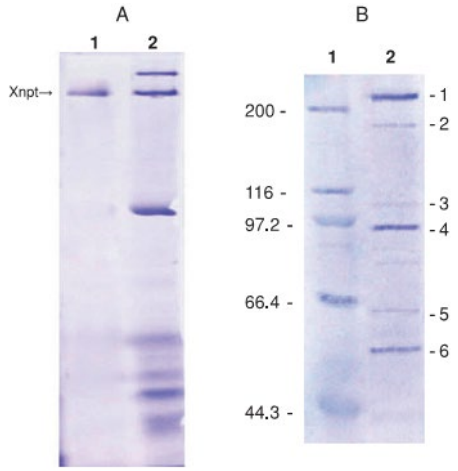

Fig. 1. Native-PAGE and SDS–PAGE analysis of Xnpt complex

A: 1: the arrow indicates Xnpt complex. 2: multi-bands of crude intracellular protein.
B: 1: molecular mass marker. 2: Xnpt complex was separated into six bands.

Table 1. Oral toxicity of Xnpt complex against H. armigera larvae (120 h)

Sample	Average weight	
	Neonate	Fourth-instar larvae
CK	9.37 ± 2.20 a*	285.6 ± 4.60 a
Xnpt complex	0.33 ± 0.01 d	133.5 ± 2.95 b

*Means followed by the same letter do not differ significantly at α= 0.05.

.

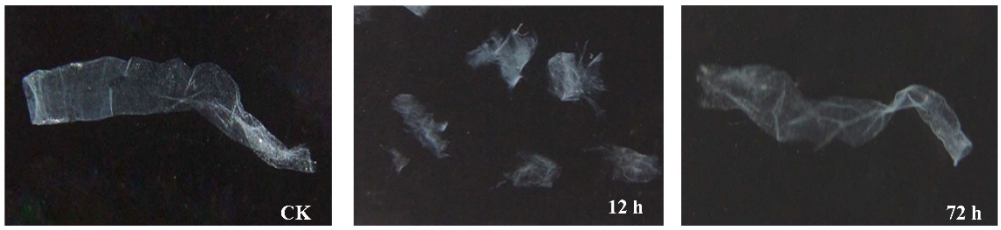

Fig. 2. The effects of Xnpt complex on the peritrophic membrane (PM) of *H. armigera*
CK: control;12h: PM after 12 h on the treated diet; 72h: PM after 72 h on the treated diet.

In the control group, the peritrophic membrane (PM) of H. armigera was complete, translucent and elastic. After 6 h of exposure to the toxin, the PMs color turned to milk-white. After 12 h, PMs ruptured into several fragments in water

(Fig. 2). However, recovery of the PMs back to the complete structure as well as transparent membrane clarity was observed after 72 h of treatment (Fig. 2).

The columnar cells were ellipsoidal and arranged closely, and PMs could be recognized clearly in control (Fig. 3). After being exposed to toxin-treated diet for 12 h, the columnar cells of treatment swelled apically and began to extrude large cytoplasmic vesicles into the gut lumen. PMs disappeared completely (Fig. 3) and although the gut epithelium was still disorganized, the PMs reappeared at 72 h (Fig.3).

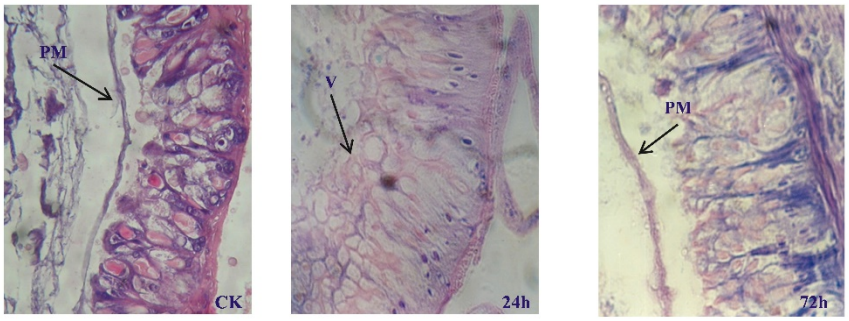

Fig. 3. The histopathological effects of Xnpt complex on the midgut of *H.armigera* (400×).
CK: control; 24h: after 24 h of exposure to Xnpt; 72h: after 72 h of exposure to Xnpt. PM: peritrophic membrane; V: vesica.

Summary

In our results, Xnpt complex with insecticidal activity was isolated from X. nematophila HB310. Xnpt showed strong growth inhibition effect on the neonates of H. armigera. The histopathological results show that the action target of the toxin complex is the midgut epithelium in H. armigera, which acted in the same fashion as tca against Manduca sexta (ffrench-Constant and Bowen, 1999; Blackburn et al., 1998) and δ-endotoxins and Vip3A from B. thuringiensis (Aronson et al., 2001). The PMs serve as the first line of defense in the midgut, so the PMs had begun to occur transformation at 6 h after being fed with toxin-treated diet and were broken into pieces after 12 h. Then, the toxin penetrated the midgut epithelial cells and continued to destroy the cells. When the insects were subjected to transient or sublethal exposure to the toxin, the epithelial cells were gradually restored and excreted, and the PMs were renewed with the disappearance of the toxin activity. Xnpt complex has high oral toxicity against a wide range of insects. Hence, it has the potential to be used as a bacterial insecticide or as an alternative to Bt for transgenic deployment.

References

Aronson, A.I. and Shai, Y. 2001. Why Bacillus thuringiensistoxins are so effective: unique features of their mode of action. FEBS Microbiology Letter, 195, 1–8.

Blackburn, M., Golubeva, E., Bowen, D. and ffrench-Constant,R.H. 1998. A novel insecticidal toxin from Photorhabdusluminescens, toxin complex a (Tca), and its histopathological effects on the midgut of Manduca sexta. Applied and Environmental Microbiology, 64, 3036–3041.

Bowen, D., Rocheleau, T. A., Blackburn, M., Andreev, O., Golubeva, E., Bhartia, R., ffrench-Constant, R. H. 1998. Insecticidal toxins from the bacterium Photorhabdus luminescens. Science, 280, 2129–2132.

French-Constant, R.H. and Bowen, D.J. 1999. Photorhabdustoxins: novel biological insecticides. Current Opinions in Microbiology, 12, 284–288.

REFINING PEST MANAGEMENT THRESHOLDS FOR WATER-DEFICIT COTTON PRODUCTION

D. Griffin
A. Randell
M. Toews
University of Georgia
Tifton, Georgia
H. Abdul
D. McCallister
K. Lewis
S. Vyavhare
M. Parajulee
Texas A&M AgriLife Research and Extension Center
Lubbock, Texas

Abstract

US cotton production takes place in the southern US under a range of irrigation deficit conditions that range from dryland to full irrigation. However, most research is conducted on well-irrigated land and there is a need to better define economic profitability models that support production under a range of conditions that address declining irrigation capacity. The objective of this project was to sequentially evaluate the impact of thrips and stink bug control under three water-deficit (zero, medium, high) conditions. Responses included pest abundance or damage during the growing season and lint fiber quality and yield at harvest. Both thrips and stink bug infestations exceeded established thresholds and representative plots were treated using insecticides. While there were profound differences in yield attributed to irrigation level, thrips infestations did not affect yield. Further, stink bug infestations significantly decreased yields under medium and high irrigation treatments, but not under dryland conditions. Fiber quality and economic assessments of yield and lint quality are pending.

World Journal of Microbiology and Biotechnology (2020) 36:56
https://doi.org/10.1007/s11274-020-02833-2

ORIGINAL PAPER

Identification of Arylphorin interacting with the insecticidal protein PirAB from *Xenorhabdus nematophila* by yeast two-hybrid system

Ziyan NanGong[1] · Xiaoxiao Guo[1] · Qing Yang[2] · Ping Song[1] · Qinying Wang[1] · Megha N. Parajulee[3]

Received: 30 October 2019 / Accepted: 18 March 2020 / Published online: 25 March 2020

Abstract

PirAB toxin was initially found in the *Photorhabdus luminescens* TT01 strain and is a demonstrated binary toxin with high insecticidal activity. In this paper, we co-expressed the *pirAB* gene of *Xenorhabdus nematophila* HB310 in a prokaryotic expression system, and we found that the PirAB protein showed high hemocoel insecticidal activity against *Galleria mellonella*, *Helicoverpa armigera* and *Spodoptera exigua.* LD_{50} values were 1.562, 2.003 and 2.17 μg/larvae for *G. mellonella*, *H. armigera*, and *S. exigua*, respectively ($p > 0.05$). Additionally, PirAB-interaction proteins were identified from *G. mellonella* by 6 × His Protein Pulldown combined with liquid chromatography–tandem mass spectrometry (LC–MS/MS). Of which, arylphorin of *G. mellonella* showed the highest matching rate. A protein domain conservative structure analysis indicated that arylphorin has three domains including Hemocyanin-N, Hemocyanin-M, and Hemocyanin-C. Among these protein domains, Hemocyanin-C has immune and recognition functions. Further, Hemocyanin-C domain of arylphorin was identified to interact with PirA but not PirB by Yeast two-hybrid system. These findings reveal, for the first time, new host protein interacting with PirAB. The identification of interaction protein may serve as the foundation for further study on the function and insecticidal mechanism of this binary toxin from *Xenorhabdus*.

Graphic Abstract

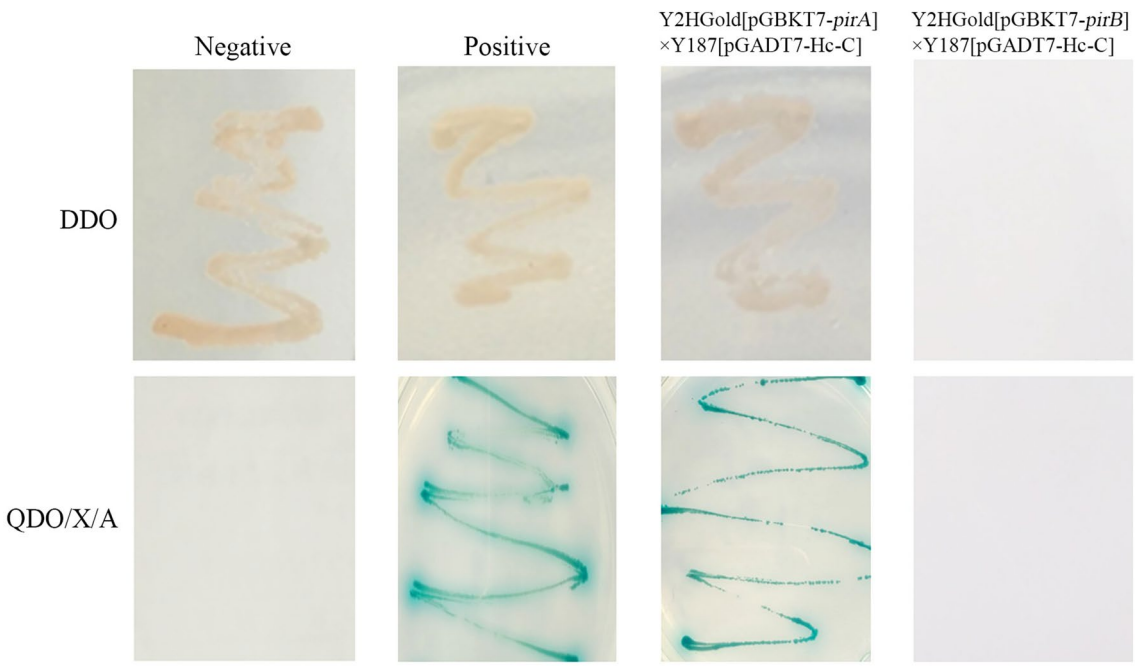

Keywords *Xenorhabdus nematophila* · PirAB toxin · His pull-down·arylphorin · Yeast two-hybrid

Extended author information available on the last page of the article

Introduction

Entomopathogenic nematodes in the field carry symbiotic bacteria (such as *Xenorhabdus* and *Photorhabdus*) into the host insect through a natural orifice or the body wall and then release the symbiotic bacteria into the blood cavity of the insect. The symbiotic bacteria multiply and release a variety of active substances, including insecticidal proteins, which can rapidly kill the host insect. In previous reports, two classes of insecticidal proteins from the symbiotic bacteria were the primary focus on their action modes. One group of insecticidal proteins are activated upon injection such as Mcf (Daborn et al. 2002), Txp40 (Brown et al. 2006), RTX (Satchell et al. 2011), and hemolysin (Brillard et al. 2001). The second group of insecticidal proteins has oral activity, such as Tc (Bowen et al. 1998), Xpt, and XnGroEL (Morgan et al. 2001). PirAB proteins were first found in the *Photorhabdus luminescens* TT01 strain and translated at two different loci of *plu4093/plu4092* and *plu4437/plu4436*, respectively (Duchaud et al. 2003). These toxins are binary proteins that exhibit oral or injectable activities against *Galleria mellonella* (Waterfield et al. 2005; Wu and Yi 2016), *Plutella xylostella* (Blackburn et al. 2006), *Aedes aegypti*, *Culex pipiens* and *Anopheles gambiae* (Duchaud et al. 2003; Ahantarig et al. 2009). Except for *Xenorhabdus* and *Photorhabdus*, the genes encoding PirAB protein are also found in *Sodalis praecaptivus* (Clayton et al. 2016), *Vibrio parahaemolyticus* (Sirikharin et al. 2015; Lee et al. 2015; Lin et al. 2019) and *Yersina intermedia* (Hurst et al. 2016).

In addition to identifying the types of toxins, an increase in understanding is required for the interaction of proteins and the action modes. For entomopathogenic nematode symbiotic bacteria, the underlying insecticidal mechanism of toxic proteins is complex but poorly understood. By contrast, the interaction between *Bacillus thuringiensis* (Bt) toxins and the receptor proteins has been studied in greater detail. Bt is one type of biopesticides that relies on insecticidal toxins, such as Cry, Cyt, and VIP proteins, during the pathogenic process against target hosts (Raymond et al. 2010). The receptor proteins of Bt include cadherin (CAD) (Hua et al. 2014), aminopeptidase N (APN) (Bravo et al. 2004), alkaline phosphatase (ALP) (Zúñiga-Navarrete et al. 2013), glycolipids (Griffitts et al. 2003), $ABCC_2$ (Zhou et al. 2016; Xiao et al. 2014), and actin (Krishnamoorthy et al. 2007), among others.

In a previous study, we confirmed that the assembly of *pir*A and *pir*B genes were essential for exhibiting hemocoel insecticidal activity against *G. mellonella* larvae (Yang et al. 2017). In this study, *pir*A and *pir*B genes of *X. nematophila* HB310 were co-expressed in a prokaryotic expression system, and the bioactivity of the recombinant PirAB protein was determined against three types of lepidopteran larva. The putative interaction proteins of PirAB were identified in *G. mellonella* by 6×His protein pulldown assay and liquid chromatography–tandem mass spectrometry (LC–MS/MS). The interaction between PirA/PirB and interaction protein was verified by the Yeast two-hybrid (Y2H) system. The results will provide a valuable theoretical basis for further studies on the function and the insecticidal mechanism of PirAB.

Materials and methods

Insects and bacteria

The insects *G. mellonella*, *H. armigera* and *S. exigua* larvae were obtained from the Pest Biocontrol Laboratory (PBL), Hebei Agricultural University, China. The lepidopteran larvae were reared on an artificial diet at 29 °C and 70% RH under a 14 h light: 10 h dark photoperiod.

The bacterium *X. nematophila* HB310 strain was isolated and stored at PBL. Broth cultures were grown from a single primary phase colony in an LB medium at 28 °C on a shaker at 200 rpm. *Escherichia coli* DH5α and BL21 (DE3) (Novagen, USA) were cultured at 37 °C for gene cloning and protein expression, respectively.

Purification and insecticidal activity measurement of PirAB protein

We purified the recombinant PirAB protein (N-terminally fused 6×His Tag) from *E. coli* BL21 (DE3) upon expression from a recombinant expression vector pET28a-*pir*AB (Yang et al. 2017). The purification of the fusion proteins and western blotting were performed as described in Yang et al. (2017).

We had known that PirAB protein did not have oral activity against *G. mellonella* larvae. Therefore, only the hemocoel insecticidal activity of the purified recombinant PirAB protein was determined by the injectable bioassay method. Five microliters of the purified PirAB protein (at 1 μg/μL) was injected directly into the hemocoel of fifth-instar larvae of *G. mellonella* and fourth-instar larvae of *H. armigera* and *S. exigua*. The control group was injected with the same dose of phosphate buffered saline (PBS, 2 mM KCl, 135 mM NaCl, 1.7 mM KH_2PO_4, 10 mM Na_2HPO_4, pH 7.4). Each larvae was injected with a sterile stainless-steel needle to prevent cross-contamination. After injection, the larvae were incubated at 28 °C on an artificial diet. The changes in morphology were monitored for 3 days. The bioassay was performed three times. A minimum of 60 larvae was used for each test. The LD_{50} values and 95% confidence limits were calculated by probit analysis.

Screening the interaction proteins of PirAB using 6 × His protein pulldown

Healthy fifth-instar larvae of *G. mellonella* were placed in a pre-chilled mortar, quickly ground to a powder in liquid nitrogen and solubilized in 200 µL protein extracting buffer (4% 3-[(3-Cholamidopropyl) dimethylammonio] propanesulfonate (CHAPS), w/v, pH 7.5; 8 mol/L carbamide, w/v, pH 7.5; 4% Dithiothreitol (DTT), w/v, pH 7.5) on ice for 30 min. After centrifugation at 13,000×*g* for 5 min at 4 °C, the soluble total tissue proteins were quantified using the Bradford method with bovine serum albumin (BSA) as the standard and stored at − 80 °C.

PirAB protein was bound to the Ni-column. The bottom of the column was blocked with a plug after PirAB was washed with imidazole. Then, the tissue proteins from *G. mellonella* were added to the Ni-column for incubation with the purified PirAB for 5 h at 4 °C. The unbound proteins were removed by washing with 200 µL wash buffer (5 mM Tris–HCl, pH 7.5, 200 mM NaCl, 1 mM DTT, and 1 mM EGTA) four times. The bound proteins were eluted twice with 20 µL elution buffer (0.5 M NaCl, 20 mM Tris–HCl, 300 mM imidazole). The eluted proteins were separated by SDS-PAGE (12%) and visualized by Coomassie Blue staining. The blank Ni-column coupled only with insect tissue proteins was used as the negative control.

After staining by Coomassie blue, the SDS-PAGE gels were cut into several strips and stored separately in 1.5 mL tubes. The gel strips were washed twice with sterile water and destainer (50% acetonitrile, 25 mM ammonium bicarbonate), respectively. The gel strips were sent to Huada Protein Research Center (HPRC) for LC–MS/MS analysis. Mascot MS/MS Ion Search (https://www.matrixscience.com) was employed for protein identification. Search parameters provided by HPRC were as follows: enzyme—trypsin; fixed modifications—carboxymethyl (C); variable modifications—Gln > pyro-Glu (N-term Q) and oxidation (M); mass values—monoisotopic; protein mass—unrestricted; peptide mass tolerance—± 0.05 Da; fragment mass tolerance—± 0.1 Da; max missed cleavages—1; instrument type—ESI-QUAD-TOF; number of queries—2557. Peptide score distribution ions score was − 10log (P), where P is the probability that the observed match is a random event. Individual ions scores > 36 indicate identity or extensive homology ($P < 0.05$).

Clone and bioinformatic analysis of the interaction protein gene

The target protein with the highest species consistency was selected as the putative interaction protein for the next confirmation. Total RNA was extracted from *G. mellonella* by using TRIzol Reagent following the manufacturer's protocol (Invitrogen, Carlsbad, USA). One microgram of total RNA was reverse-transcribed into cDNA using 1st strand cDNA Synthesis kit (TaKaRa, Dalian, China). The reverse system was composed of: Total RNA 2 µL, 5 × All-In-One RT MasterMix 4 µL, molecular graded water was add to adjust the reaction mixture to 20 µL. The reverse conditions were as follows: at 25 °C for 10 min followed by at 42 °C for 50 min, and a final extension step at 85 °C for 5 min.

According to the gene sequence information of the interaction protein in GenBank (Access No. AAA74229.1), the primers with restriction enzyme cutting sites were designed (Table 1). These primers were synthesized in Sangon Biotech (Shanghai, China). The PCR product was purified and double-digested, following which, the plasmid was extracted and inserted into the pMD18-T vector (TaKaRa, Dalian, China) and then sequenced. The bioinformatic analysis of the target gene was performed in the next step.

Construction of the hybrid plasmids for yeast two-hybrid

The plasmids pMD18-*pir*A and pMD18-*pir*B kept in our laboratory were digested with restriction enzymes and then ligated into pGBKT7 vector between EcoRI and BamHI sites, respectively, designated pGBKT7-*pir*A and pGBKT7-*pir*B. They were transformed into *E. coli* DH5α (Transgen, Beijing, China) and verified by endonuclease cleavage and sequencing (Sangon Biotech, Shanghai, China).

The coding sequence of target gene was amplified with a special primer pair (Table 1) and purified using a Gel Extraction Kit (Takara, Dalian, China). The PCR products

Table 1 Synthetic primers for plasmid construction of pMD18T-ary and pGADT7-Hc-C

Plasmid	Primers	Sequence (5′–3′)	Restriction enzyme sites
pMD18T-ary	Ary-F	5′-CC*ATCGAT*ATGCAGACTGTCCTCTTTTTAGC-3’	ClaI
	Ary-R	5′-CG*GGATCC*TTAGTGGTTAGAGACTTGGTTCTGGC-3’	BamHI
pGADT7-Hc-C	Hc-c F	5′-CC*ATCGAT*GCCCTTATTCTCAAGATGTACT-3’	ClaI
	Hc-c R	5′-CG*GGATCC*ATAAACATAAACATCCTTGAA-3’	BamHI

ary arylphorin, *Hc-C* hemocyanin-C domain of arylphorin

and pGADT7 were digested and connected to construct the hybrid plasmid. The hybrid plasmid would be identified by restriction enzyme digestion and sequencing.

Auto-activation and toxicity detection

Auto-activation and toxicity detection of the recombinant plasmids were done according to the instructions of Matchmaker™ Gold Yeast Two-Hybrid System. The pGBKT7-*pir*A and pGBKT7-*pir*B plasmids were transformed into the yeast strain Y2HGold, respectively. Transformants were then grown on SD/-Trp (40 μg/mL X-α-Gal) and SD/-Trp/X/A (40 μg/mL X-α-Gal and 125 ng/mL aureobasidin A) agar plates for 3–5 days. The pGBKT7 empty vector was also transformed into Y2HGold competent cells as a control. Lack of autoactivation was indicated by white colonies on SD/-Trp and SD/-Trp/X plates and the absence of colony growth on SD/-Trp/X/A plates. The plasmids that did not possess autoactivation activity were used in the yeast two-hybrid system.

By the same method, the empty pGADT7 and recombinant pGADT7 plasmid were transformed into yeast strain Y187 and the growth of them on SD/-Leu, SD/-Leu/X, and SD/-Leu/X/A plates were observed.

Interaction verification of PirA/PirB with the interaction protein fragment

The yeast strain Y2HGold containing the plasmids pGBKT7-*pir*A and pGBKT7-*pir*B were inoculated into SD/-Trp liquid medium, respectively. After centrifuging, the culture was prepared with 4 mL liquid medium SD/-Trp to resuspend the sedimentation (the cell concentration was more than 1.0×10^8 cell/mL). In the next step, 1 mL of Y187 with recombinant pGADT7 plasmid contained the interaction protein gene fragment (the titer with 42.0×10^7 cfu/mL) and 4–5 mL of Y2HGold were fused in a sterile flask, then 45 mL liquid medium 2 × YPDA was added and incubated at 30 °C with 50 rpm for 20 h. The fusion process was observed in the phase contrast microscope. When the binders were formed, the fusion culture was coated on the selective medium SD/-Trp, SD/-Leu, and SD/-Trp-Leu plates, respectively, and cultured inversely for 5 d at 30 °C. Then, the binding rate was determined after calculating the number of yeast colonies. The remaining fusion culture was coated on the selective medium SD/-Trp/-Leu/X-α-Gal/AbA (DDO/X/A) 200 μL per plate and cultured for 5 days at 30 °C. Blue yeast colonies on this selective medium were coated on higher stringency SD/-Trp/-Leu/-Ade/X-α-Gal/AbA (QDO/X/A) agar plates. The blue yeast colonies on this selective medium was scored as potential positive interactions. These screening for interactions were carried out independently at least twice. The blue yeast colonies on the medium QDO/X/A were picked and transferred to the high screening rate medium QDO/X/A by screening repeatedly to identify the positive interactions. Y2HGold [pGBKT7-Lam] × Y187[pGADT7-T] and Y2HGold [pGBKT7-p53] × Y187 [pGADT7-T] were cultured as negative and positive control, respectively.

Results

Heterologous expression and insecticidal activity of PirAB toxin

BL21 (pET28a-*pir*AB) strain carrying the recombinant plasmid was induced by IPTG. The recombinant PirAB protein was presented in SDS-PAGE gel (48 kDa for PirB and 17 kDa for PirA, Fig. 1a, lane 6). After purification, the recombinant PirAB protein was verified with a commercial anti-His-tagged mouse monoclonal antibody (Fig. 1b).

The immune response in insect host to PirAB protein was quantified on full-grown larvae (4–5 instars) of three selected lepidopteran species (*G. mellonella*, *H. armigera*, and *S. exigua*) via injection bioassay. After ultrafiltration concentration and purification, the injection of the recombinant protein with 5 μg/larva caused 100% mortality within 48 h in all three lepidopteran species. The base mortality of *G. mellonella*, *H. armigera*, and *S. exigua* larvae during the bioassay was less than 5% in control injected with PBS. A low-dose injection bioassay with PirAB protein (2.5 μg/larva) still showed high injectable insecticidal activity against three host insects (Fig. 2). Compared with the other two host insects, the larva of *G. mellonella* was more sensitive to PirAB protein. Before death, the larvae usually became less vital and shrunk in size. The entire body gradually turned dark brown during the process when the larvae became moribund. The LD_{50} of PirAB against *G. mellonella*, *H. armigera*, and *S. exigua* were 1.562, 2.003 and 2.17 μg/larva, respectively (Table 2).

Detection and identification of PirAB: interaction proteins

After incubation with insect tissue proteins, the potential interaction proteins with PirAB were resolved in SDS-PAGE. The gel was divided into nine regions ranging in molecular size from 15 to 100 kDa (except for PirA and PirB, as shown in Fig. 3, lane 2, the gel was divided into nine regions named as PD1-PD9). These nine regions of the gel were cut and analyzed separately by LC–MS/MS spectrum analysis. The negative control was the Ni-column blocked and coupled only with insect tissue proteins and without PirAB protein, and no protein band was observed after SDS-PAGE analysis (Fig. 3, lane 3).

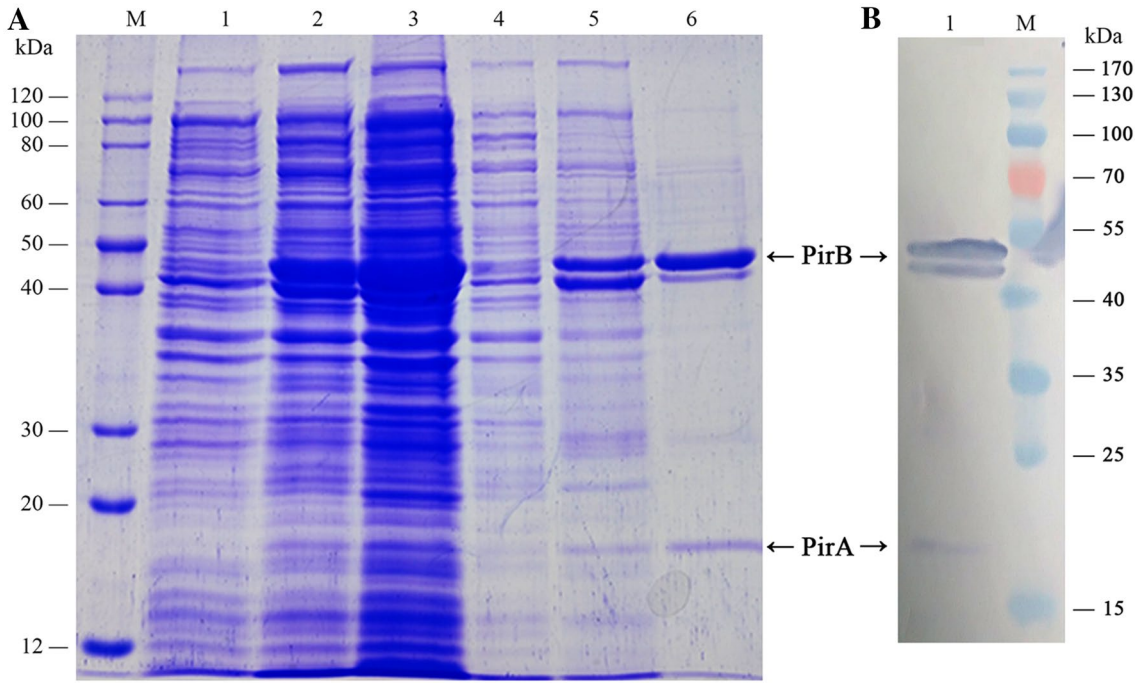

Fig. 1 SDS-PAGE and western blot analysis of the recombinant PirAB protein. **a** SDS-PAGE gel of PirAB stained with Coomassie Blue (12% gel). M: high-range marker; 1: bacterial cell lysate from a non-induced bacterial culture; 2: soluble lysates of BL21 (pET28a-*pir*AB) from an IPTG-induced culture; 3: insoluble lysates of BL21 (pET28a-*pir*AB) from an IPTG-induced culture; 4: flow through solution after binding; 5: purified PirAB with 60 mM imidazole; 6: purified PirAB with 300 mM imidazole. **b** Western blot analysis of PirAB with anti-PirAB antibodies. M: pre-stained protein marker; 1: PirAB protein. Arrow indicates the recombinant protein band

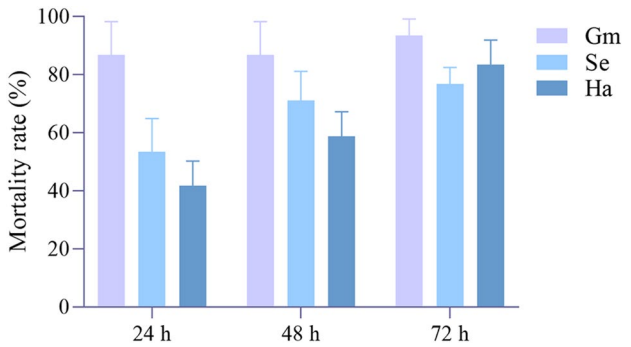

Fig. 2 The injectable effects of PirAB against the larvae of *G. mellonella*, *H. armigera*, and *S. exigua*. Concentrations of the proteins were 2.5 μg/larvae. Each treatment was replicated independently three times with 20 larvae each. Error bars represent the standard deviation of three replications. Mortality was recorded after 24 h, 48 h and 72 h of exposure. *Gm G. mellonella*, *Ha H. armigera*, *Se S. exigua*

The corresponding uniproteins of these protein bands were identified in NCBI non-redundant protein sequences database. The data in Table 3 show a list of the putative interaction proteins from *G. mellonella* with the top matching rate using a significance score higher than 50 as the threshold. Arylphorin and hexamerin of *G. mellonella* were identified as PirAB—interaction protein detected in PD-1, PD-2, PD-3, PD-4, PD-7 and PD-8 bands, which had the highest significance score in the LC–MS/MS analysis. Additionally, ferritin and actin were also detected.

Clone and bioinformatic analysis of arylphorin

Arylphorin, showing the highest matching rate in the protein identification results, was selected for the further characterizations. After RT-PCR using a specific primer, arylphorin protein gene of approximately 2109 bp was generated, which encoded 702 aa (molecular weight of 83.7 kDa) (Fig. 4). Sequencing and alignment results revealed that the nucleotide sequence identity exceeded 99% similarity with the reference strain.

A protein domain conservative structure analysis indicated that arylphorin has three domains, which included Hemocyanin-N, Hemocyanin-M, and Hemocyanin-C (Fig. 4). The aromatic protein domain Hemocyanin-C (named as Hc-C in this paper) has immune and recognition functions, which was then selected as the research object. To identify whether PirA/PirB of *Xenorhabdus* and Hc-C from *G. mellonella* interact physically, the interaction between PirA/PirB protein and domain Hc-C would be verified by the yeast two-hybrid system.

Table 2 The LD_{50} values for PirAB against *Galleria mellonella*, *Helicoverpa armigera* and *Spodoptera exigua*

Test insect	LD_{50} (μg/larvae)	r	Regression equation	95% confidence limits (μg/mL)
G. mellonella	1.562	0.961	y = 5.519x − 1.068	1.443–1.670
H. armigera	2.003	0.935	y = 4.588x − 1.384	1.851–2.165
S. exigua	2.17	0.965	y = 2.465x − 0.829	1.577–3.092

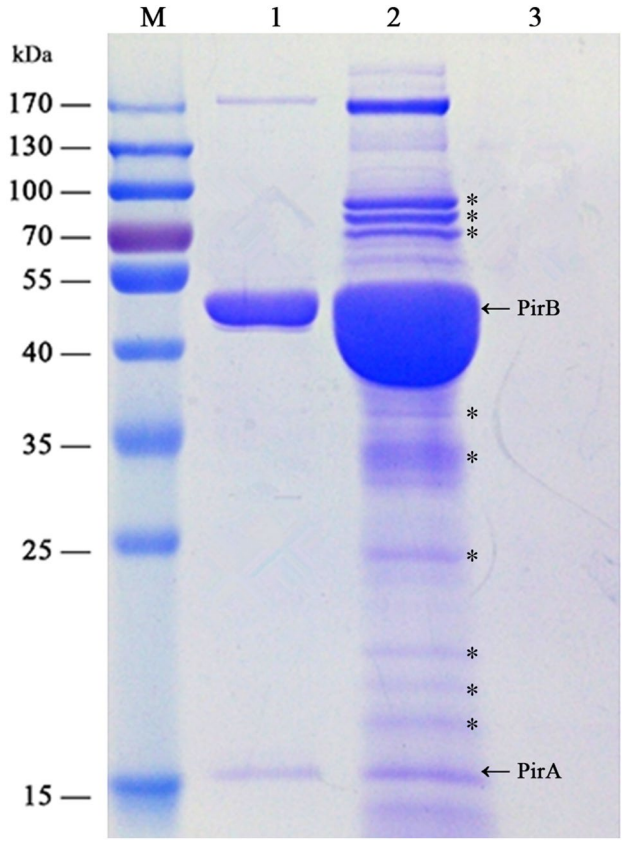

Fig. 3 Identification of PirAB-interaction proteins in the total tissue proteins from *G. mellonella* using the His-pulldown method. M: pre-stained protein marker; 1: PirAB protein; 2: insect proteins from *G. mellonella* in Ni-column incubated with PirAB protein, the bands denoted by an asterisk from the top to the bottom are named as PD1-9, the arrow indicates PirA and PirB protein bands; 3: control sample in Ni-column with only insect tissue proteins

Construction, auto-activation and toxicity detection of the hybrid plasmids

The Hc-C gene fragment encoding a 233-residue peptide (Fig. 4) was PCR amplified, digested and connected with pGADT7 to construct the plasmid pGADT7-Hc-C. Positive recombinant plasmid pGADT7-Hc-C was identified by BamHI and ClaI restriction enzyme digestion, which displayed 8.0 kb and 700 bp gene fragments, respectively (Fig. 5). The pGBKT7-*pir*A and pGBKT7-*pir*B plasmids were constructed as described in methods and identified by EcoRI and BamHI incision enzyme digestion, which displayed 7.3 kb, 408 bp and 1290 bp fragments, respectively, as expected (Fig. 5).

To test the autoactivation activity of the proteins in yeast cells, the pGBKT7-*pir*A and pGBKT7-*pir*B plasmids were transformed into Y2HGold cells, and subsequently, the transformants were grown on SD/-Trp, SD/-Trp/X-α-Gal, and SD/-Trp/AbA/X-α-Gal. The results showed that no autoactivation activity was detected from PirA and PirB (Table 4). Furthermore, the colony size of Y2HGold [pGBKT7-*pir*A] or Y2HGold [pGBKT7-*pir*B] was similar to that of the negative control yeast strain Y2HGold [pGBKT7]. The fusion proteins expressed in Y2HGold [pGBKT7-*pir*A] and Y2HGold [pGBKT7-*pir*B] showed no toxic effect to the yeast strain Y2HGold.

After the plasmid pGADT7-Hc-C was successfully transformed into the yeast cell Y187, the yeast strain Y187 [pGADT7-Hc-C] grew the milky white colonies on the medium SD/-Leu, very pale blue colonies on the medium SD/-Leu/X-α-Gal, and no colony on the medium SD/-Leu/AbA/X-α-Gal (Table 4). The yeast strain Y187 [pGADT7-Hc-C] and the negative control yeast strain Y187 [pGADT7] with the same dilution grew the milky white colonies with the same size. The results showed that no autoactivation and toxic activity was detected from pGADT7-Hc-C.

Interaction detection of PirA/PirB with the interaction protein fragment

The plasmid pGADT7-Hc-C and pGBKT7-*pir*A/pGBKT7-*pir*B were mixed and incubated on SD/-Leu/-Trp (DDO) medium and SD/-Ade/-His/-Leu/-Trp/X-α-Gal (QDO/X) medium, respectively. Co-transformation of pGBKT7-53 and pGADT7-T was used as positive controls and pGBKT7-Lam and pGADT7-T as negative controls. The positive control showed blue colonies, whereas negative control showed no colony on QDO/X/A plates (Fig. 6). Protein interactions were monitored by comparing the growth and color of the yeast with the positive and negative controls. The yeast strain Y2H gold harboring pGBKT7-*pir*A and pGADT7-Hc-C grew well in the medium lacking tryptophan and leucine and formed clear blue colonies in QDO/X medium. Therefore, PirA was verified to interact with Hc-C domain

Table 3 The LC–MS/MS assay results of binding proteins to PirAB on total tissue proteins from *Galleria mellonella* by His pull-down

Fraction	Top match[a]		Accession number	Mr	Score	Sequence coverage (%)
PD-1	Hexamerin	*Galleria mellonella*	gil347090	81,800	1437	27
PD-2	Arylphorin	*Galleria mellonella*	gil159078	83,651	1307	39
PD-3	Hexamerin	*Galleria mellonella*	gil347090	81,800	268	16
PD-4	Hexamerin	*Galleria mellonella*	gil347090	81,800	206	8
PD-5	Actin (Fragment)	*Mayetiola destructor*	gil719555623	24,572	55	7
PD-6	Ferritin	*Galleria mellonella*	gil17901818	26,727	386	18
PD-7	Hexamerin	*Galleria mellonella*	gil347090	81,800	189	4
PD-8	Hexamerin	*Galleria mellonella*	gil347090	81,800	122	6
PD-9	Ferritin	*Galleria mellonella*	gil11890404	23,932	744	37

[a]All matches were to sequences from *G. mellonella*

of arylphorin from *G. mellonella* (Fig. 6). Compared to the results of the control, there was no interaction between PirB and Hc-C domain of arylphorin.

Discussion

The PirAB toxin was found originally in *P. luminescens*. It showed both injectable and oral insecticidal activities against larvae of Lepidoptera (Waterfield et al. 2005) and Diptera (Duchaud et al. 2003; Ahantarig et al. 2009). In our research, we only found the injectable insecticidal activities of PirAB toxin from *X. nematophila* against three types of lepidopteran larvae. Furthermore, PirAB showed greater insecticide activity against *G. mellonella* than *H. armigera* and *S. exigua*.

Identification and characterization of the interaction proteins is important for understanding the insecticidal mechanism of toxin protein. Several binding proteins (e.g., APN, ALP, cadherin and ABCC) of Bt Cry toxin were previously identified in different insects (Banks et al. 2001; Arenas et al. 2010; Xiao et al. 2014; Zhou et al. 2016). Here, three proteins including arylphorin, hexamerin and ferritin from *G. mellonella* that supposedly interacted with the PirAB toxin by 6 × His pulldown method. Hexamerin has been functionally classified as larval storage proteins (Telfer and Kunkel. 1991). Also, hexamerin is highly expressed in the immune processes of Diptera (Poopathi et al. 2014), Coleoptera (Kim et al. 2003), Lepidoptera (Telfer et al. 1983) and Hemiptera (Eliautout et al. 2016). Typically, the hexamerin subunits have masses in the range of about 80 kDa, giving rise to a native molecule of about 500 kDa. Previous report have suggested that hexamerin fall into four categories: lepidopteran methionine rich proteins, lepidopteran arylphorin, certain lepidopteran juvenile hormone-suppressible proteins, and the dipteran storage proteins (Telfer and Kunkel 1991). Among them, arylphorin which contains a high proportion of aromatic amino acids with phenylalanine and tyrosin, is generally found during the latter part of the larval stage in holometabolous insects. Arylphorin also plays a central role in insect immunity (Beresford et al. 1997; Castagnola et al. 2017). For example, the expression of arylphorin and apolipoprotein increased significantly in *G. mellonella* infected by bacteria (Fallon et al. 2011). Based on the results from this study, we postulate that PirAB toxin might cause an immune response by the aromatic proteins, affecting arylphorin in the hemocoel.

The interaction mode of PirA and PirB of *Xenorhabdus* has not yet been determined. However, the model of PirA*vp*/PirB*vp* from *V. parahaemolyticus* provides insight for the further understanding the interaction interface between PirA and PirB from *Xenorhabdus. V. parahaemolyticus* (Lee et al. 2015), *Vibrio campbellii* (Dong et al. 2017), *Vibrio punensis* (Restrepo et al. 2018) and *Micrococcus luteus* (Durán-Avelar et al. 2018) also harbor the *pir*A and *pir*B toxin genes, which are homologs of the *Photorhabdus* insect-related (Pir) binary toxins. The researchers proposed a heterotetrameric interaction model of this binary toxin complex and implied that the components have a low binding affinity based on the results of isothermal titration calorimetry (ITC), gel filtration, cross-linking and hydrogen–deuterium exchange (HDX) mass spectrometry (Lin et al. 2019). In addition to showing that PirA*vp* and PirB*vp* form a complex, they also found that the assembled PirA*vp* and PirB*vp* structure was similar to *Bt* Cry insecticidal toxins, and speculated that PirA*vp*/PirB*vp* toxins might use a similar mechanism to damage host cells as Cry toxins (Lee et al. 2015; Lin et al. 2017). Recently, some researchers proposed that PirA*vp* recognizes and binds with a receptor on the host cell membrane, after which the newly-exposed N-terminus region of PirB*vp* is pulled toward the cell membrane where it inserts into the membrane using its α-helix and initiates the process of pore formation (Lin et al. 2019).

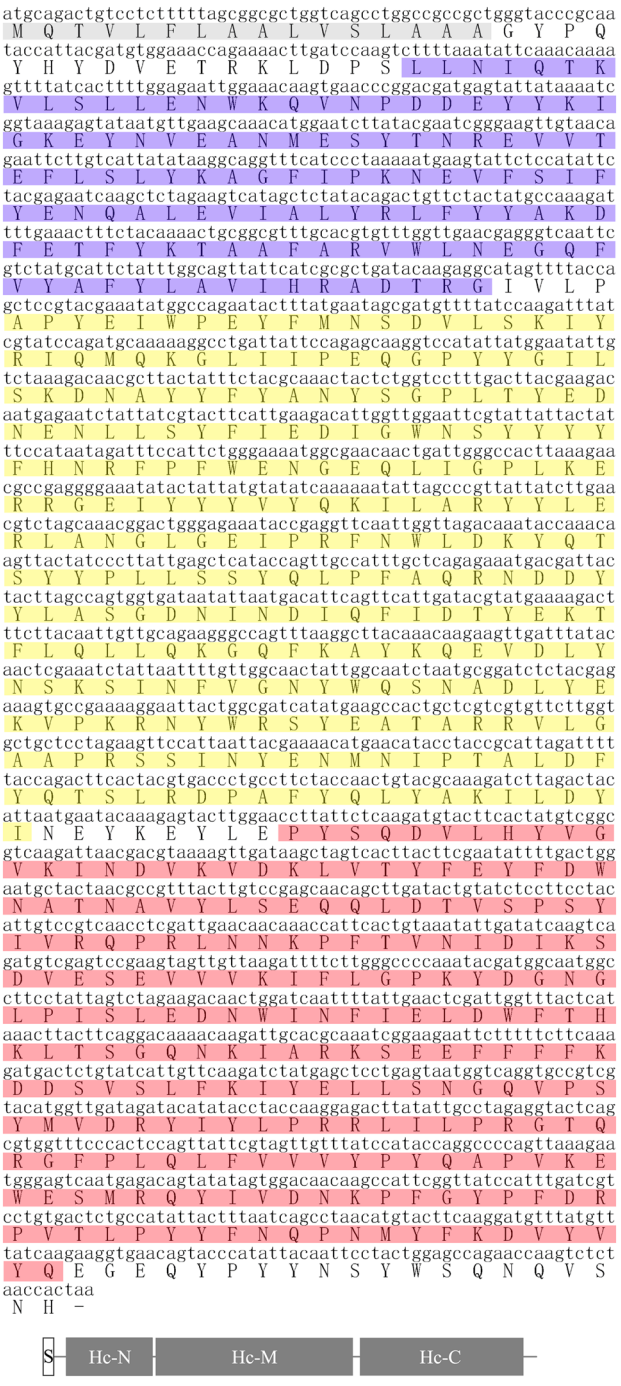

Fig. 4 Sequence alignment and protein domain conservative structure of arylphorin. The protein domain sequences of arylphorin are aligned using Clustal alignment (www.ebi.ac.uk/Tools/msa/clustalo/). The signal peptide is shown in gray. The alignment of Hemocyanin-N domain is indicated by the purple color. The Hemocyanin-M motif is shaded in yellow. The Hemocyanin-C motif is marked in pink. The positions of these protein domains are as follows: Hemocyanin-N, 34 to 156; Hemocyanin-M, 163 to 440; Hemocyanin-C, 450 to 681

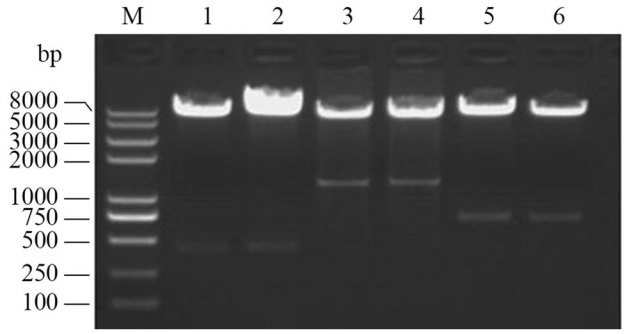

Fig. 5 Identification of double enzyme digestion of pGBKT7-*pirA*, pGBKT7-*pirB* and pGADT7-Hc-C. 1,2: pGBKT7-*pirA* was identified by EcoRI and BamHI digestion, which display 7.3 kb and 408 bp fragments; 3,4: pGBKT7-*pirB* was identified by EcoRI and BamHI digestion, which display 7.3 kb and 1290 bp fragments; 5,6: pGADT7-Hc-C was identified by BamHI and ClaI restriction enzyme digestion, which displays 8.0 kb and 700 bp gene fragments. M: Trans 2 K Plus II DNA Marker

We have previously confirmed that the co-existence of PirA and PirB is necessary for their insecticidal activity (Yang et al. 2017). However, the binding of the toxin protein with the host interaction protein does not necessarily require both of PirA and PirB. In this paper, PirA was identified to interact with Hc-C domain of arylphorin from *G. mellonella*. There was no interaction between PirB and Hc-C domain of arylphorin. Thus, our results supported the interaction model of this binary toxin complex and hypothesized that the binary toxin may recognize and bind to the receptor via PirA. After receptor binding, PirB may play a further destructive role, which warrants further investigation.

Our results indicated that PirAB toxin had significant intraperitoneal injection activity against *G. mellonella*, *H. armigera* and *S. exigua*. Using 6 × His pulldown, we found several *G. mellonella* proteins that interacted with PirAB toxin. More specifically, PirA can interact with Hc-C domain of arylphorin from *G. mellonella*. Therefore, arylphorin is a putative interaction protein of *X. nematophila* PirAB toxin. Results from this study greatly enhances our understanding of the insecticidal mechanism of PirAB and the opportunity to utilize these potent insecticidal proteins as plant incorporated proteins in integrated crop pest management. Further studies are required to characterize these interactions and verify whether they are involved in PirAB toxicity to insect hosts.

Table 4 Detection of autoactivation and toxicity of plasmids pGBKT7-*pirA*, pGBKT7-*pirB* and pGADT7-Hc-C

Type	SD/-Trp/X	SD/-Trp/X/A	SD/-Leu/X	SD/-Leu/X/A	DDO/X/A	MEL1	AUR1-C
pGADT7-Hc-C	/	/	+	/	/	White	No
pGBKT7-*pirA*	+	−	/	/	/	White	No
pGBKT7-*pirB*	+	−	/	/	/	White	No
Positive control	/	/	/	/	+	Blue	Yes
Negative control	/	/	/	/	−	None	No

X x-α-gal, *A* AbA, / without cultivation, + growth, − no growth, *DDO* SD/-Ade/-His/-Leu/-Trp plates MEL1, no AUR1-C

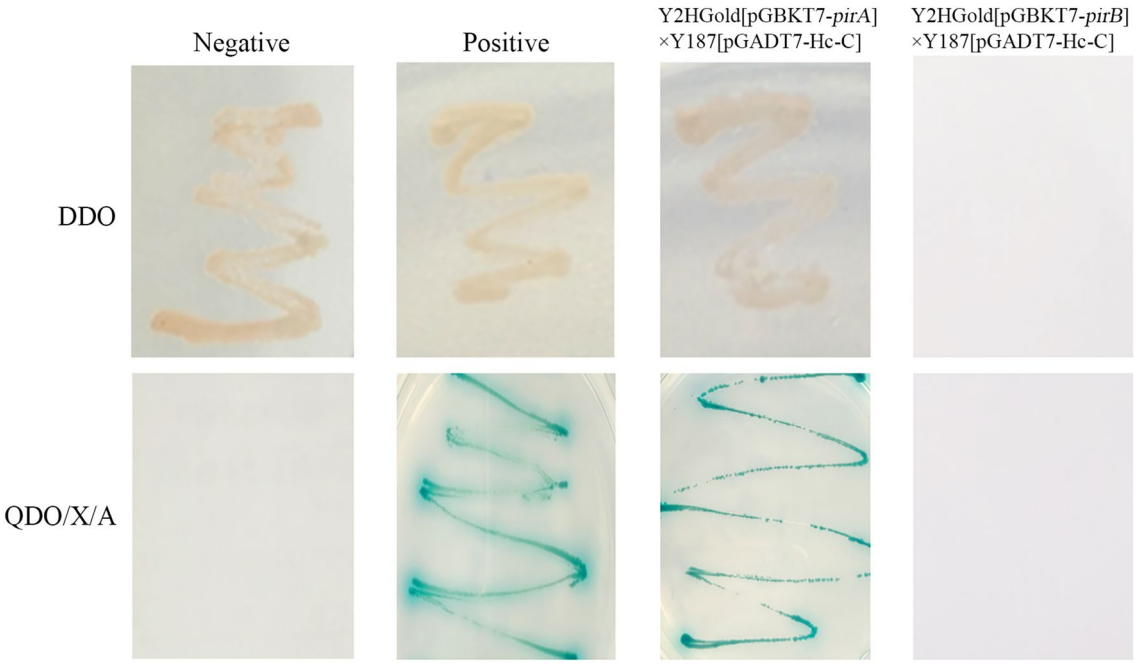

Fig. 6 Interaction PirA/PirB with Hc-C domain of arylphorin. Co-transformation of pGBKT7-53 and pGADT7-T was used as positive control and pGBKT7-Lam and pGADT7-T as negative control. The positive control showed blue colonies, whereas negative control showed no colony on QDO/X/A plate. Positive interactions showed the presence of blue colonies on QDO/X/A plate

Acknowledgements The Natural Science Foundation of Hebei Province of China (C2016204107) provided financial support for this study.

Compliance with ethical standards

Conflict of interest The authors declare no conflict of interest.

References

Ahantarig A, Chantawat N, Waterfield NR, Ffrenchconstant R (2009) PirAB toxin from *Photorhabdus asymbiotica* as a larvicide against dengue vectors. Appl Environ Microbiol 75:4627–4629. https://doi.org/10.1128/AEM.00221-09

Arenas I, Bravo A, Soberón M, Gómez I (2010) Role of alkaline phosphatase from *Manduca sexta* in the mechanism of action of *Bacillus thuringiensis* Cry1Ab toxin. J Biol Chem 285:12497–12503. https://doi.org/10.1074/jbc.M109.085266

Banks DJ, Jurat-Fuente JL, Dean DH, Adang MJ (2001) *Bacillus thuringiensis* Cry1Ac and Cry1Fa delta-endotoxin binding to anovel 110 kDa aminopeptidase in *Heliothis virescens* is not *N*-acetylgalactosamine mediated. Insect Biochem Mol Biol 31:909–918. https://doi.org/10.1016/s0965-1748(01)00038-8

Beresford PJ, Basinski-Gray JM, Chiu JK, Chadwick JS (1997) Characterization of hemolytic and cytotoxic gallysins: a relationship with arylphorins. Dev Comp Immunol 21:253–266. https://doi.org/10.1016/s0145-305x(97)00011-6

Blackburn MB, Farrar RR, Novak NG, Lawrence SD (2006) Remarkable susceptibility of the diamondback moth (*Plutella xylostella*) to ingestion of Pir toxins from *Photorhabdus luminescens*. Entomol Exp Appl 121:31–37. https://doi.org/10.1111/j.1570-8703.2006.00457.x

Bowen D, Rocheleau TA, Blackburn M, Andreev O (1998) Insecticidal toxins from the bacterium *Photorhabdus luminescens*. Science 280:2129–2132. https://doi.org/10.1126/science.280.5372.2129

Bravo A, Gomez I, Conde J, Munoz-Garay C (2004) Oligomerization triggers binding of a *Bacillus thuringiensis* Cry1Ab pore-forming toxin to aminopeptidase N receptor leading to insertion into membrane microdomains. Biochim Biophys Acta 1667:38–46. https://doi.org/10.1016/j.bbamem.2004.08.013

Brillard J, Ribeiro C, Boemare N, Brehélin M (2001) Two distinct hemolytic activities in *Xenorhabdus nematophila* are active against immunocompetent insect cells. Appl Environ Microbiol 67:2515–2525. https://doi.org/10.1128/AEM.67.6.2515-2525.2001

Brown SE, Cao AT, Dobson P, Hines ER (2006) Txp40, a ubiquitous insecticidal toxin protein from *Xenorhabdus* and *Photorhabdus* bacteria. Appl Environ Microbiol 72:1653–1662. https://doi.org/10.1128/AEM.72.2.1653-1662.2006

Clayton AL, Jackson DG, Weiss RB, Dale C (2016) Adaptation by deletogenic replication slippage in a nascent symbiont. Mol Biol Evol 33:1957–1966. https://doi.org/10.1093/molbev/msw071

Castagnola A, Jackson J, Perera OP, Oppert C, Eda S, Jurat-Fuentes JL (2017) Alpha-arylphorin is a mitogen in the *Heliothis virescens* midgut cell secretome upon Cry1Ac intoxication. Peer J 5:e3886. https://doi.org/10.7717/peerj.3886

Daborn PJ, Waterfield N, Silva CP, Au CPY (2002) A single *Photorhabdus* gene, makes caterpillars floppy (mcf), allows *Escherichia coli* to persist within and kill insects. PNAS 99:10742–10747. https://doi.org/10.1073/pnas.102068099

Dong X, Wang H, Xie G, Zou P, Guo C, Liang Y, Huang J (2017) An isolate of *Vibrio campbellii* carrying the *pir*VP gene causes acute hepatopancreatic necrosis disease. Emerg Microbes Infect 6:e2. https://doi.org/10.1038/emi.2016.131

Duchaud E, Rusniok C, Frangeul L, Buchrieser C (2003) The genome sequence of the entomopathogenic bacterium *Photorhabdus luminescens*. Nat Biotechnol 21:1307–1313. https://doi.org/10.1038/nbt886

Durán-Avelar MJ, Vázquez-Reyes A, González-Mercado AL, Zambrano-Zaragoza J, Ayón-Pérez F, Agraz-Cibrián JM, Gutiérrez-Franco J, Vibanco-Pérez N (2018) pirA- and pirB-like gene identification in *Micrococcus luteus* strains in Mexico. J Fish Dis 41:1667–1673. https://doi.org/10.1111/jfd.12874

Eliautout R, Dubrana MP, Vincent-Monégat C, Vallier A (2016) Immune response and survival of *Circulifer haematoceps* to *Spiroplasma citri* infection requires expression of the gene hexamerin. Dev Comp Immunol 54:7–19. https://doi.org/10.1016/j.dci.2015.08.007

Fallon JP, Troy N, Kavanagh K (2011) Pre-exposure of *Galleria mellonella* larvae to different doses of *Aspergillus fumigatus* conidia causes differential activation of cellular and humoral immune responses. Virulence 2:413–421. https://doi.org/10.4161/viru.2.5.17811

Griffitts JS, Huffman DL, Whitacre JL, Barrows BD (2003) Resistance to a bacterial toxin is mediated by removal of a conserved glycosylation pathway required for toxin-host interactions. J Biol Chem 278:45594–45602. https://doi.org/10.1074/jbc.M308142200

Hua G, Park Y, Adang MJ (2014) Cadherin AdCad1 in *Alphitobius diaperinus* larvae is a receptor of Cry3Bb toxin from *Bacillus thuringiensis*. Insect Biochem Mol Biol 45:11–17. https://doi.org/10.1016/j.ibmb.2013.10.007

Hurst MRH, Beattie A, Altermann E, Moraga RM (2016) The draft genome sequence of the *Yersinia entomophaga* entomopathogenic type strain MH96T. Toxins 8:143. https://doi.org/10.3390/toxins8050143

Kim SR, Yoon HJ, Park NS, Lee SM (2003) Molecular cloning, expression, and characterization of a cDNA encoding the arylphorin-like hexameric storage protein from the mulberry longicorn beetle, *Apriona germari*. Arch Insect Biochem Physiol 53:49–65. https://doi.org/10.1002/arch.10085

Krishnamoorthy M, Jurat-Fuentes JL, McNall RJ, Andacht T (2007) Identifcation of novel Cry1Ac binding proteins in midgut membranes from *Heliothis virescens* using proteomic analyses. Insect Biochem Mol Biol 37:189–201. https://doi.org/10.1016/j.ibmb.2006.10.004

Lee CT, Chen IT, Yang YT, Ko TP (2015) The opportunistic marine pathogen *Vibrio parahaemolyticus* becomes virulent by acquiring a plasmid that expresses a deadly toxin. PNAS 112:10798–10803. https://doi.org/10.1073/pnas.1503129112

Lin SJ, Hsu KC, Wang HC (2017) Structural insights into the cytotoxic mechanism of *Vibrio parahaemolyticus* PirAvp and PirBvp toxins. Mar Drugs 15:373. https://doi.org/10.3390/md15120373

Lin SJ, Chen YF, Hsu KC, Chen YL, Tzu Ko, Lo CF, Wang HC, Wang HC (2019) Structural insights to the heterotetrameric interaction between the *Vibrio parahaemolyticus* PirAvp and PirBvp toxins and activation of the Cry-like pore-forming domain. Toxins 11:233. https://doi.org/10.3390/toxins11040233

Morgan JAW, Sergeant M, Ellis D, Ousley M (2001) Sequence analysis of insecticidal genes from *Xenorhabdus nematophilus* PMFI296. Appl Environ Microbiol 67:2062–2069. https://doi.org/10.1128/AEM.67.5.2062-2069.2001

Poopathi S, Thirugnanasambantham K, Mani C, Mary KA (2014) Hexamerin a novel protein associated with *Bacillus sphaericus* resistance in *Culex quinquefasciatus*. Appl Biochem Biotechnol 172:2299–2307. https://doi.org/10.1007/s12010-013-0681-5

Raymond B, Johnston PR, Nielsen-LeRoux C, Lereclus D (2010) *Bacillus thuringiensis*: an impotent pathogen? Trends Microbiol 18:189–194

Restrepo L, Bayot B, Arciniegas S, Bajaña L, Betancourt I, Panchana F, Muñoz AR (2018) PirVP genes causing AHPND identified in a new *Vibrio* species (*Vibrio punensis*) within the commensal *Orientalis* clade. Sci Rep 8:13080. https://doi.org/10.1038/s41598-018-30903-x

Satchell KJ (2011) Structure and function of MARTX toxins and other large repetitive RTX proteins. Annu Rev Microbiol 65:71–90. https://doi.org/10.1146/annurev-micro-090110-102943

Sirikharin R, Taengchaiyaphum S, Sanguanrut P, Chi TD (2015) Characterization and PCR detection of binary, pir-like toxins from *Vibrio parahaemolyticus* isolates that cause acute hepatopancreatic necrosis disease (AHPND) in shrimp. PLoS ONE 10:e0126987. https://doi.org/10.1371/journal.pone.0126987

Telfer WH, Keim PS, Law JH (1983) Arylphorin, a new protein from *Hyalophora cecropia*: comparisons with calliphorin and manducin. Insect Biochem 13:601–613. https://doi.org/10.1016/0020-1790(83)90034-3

Telfer WH, Kunkel JG (1991) The function and evolution of insect storage hexamers. Annu Rev Entomol 36:205. https://doi.org/10.1146/annurev.en.36.010191.001225

Waterfield N, Kamita SG, Hammock BD, Ffrench-Constant R (2005) The *Photorhabdus* Pir toxins are similar to a developmentally regulated insect protein but show no juvenile hormone esterase activity. FEMS Microbiol Lett 245:47–52. https://doi.org/10.1016/j.femsle.2005.02.018

Wu GQ, Yi YH (2016) Haemocoel injection of PirA1B1 to *Galleria mellonella* larvae leads to disruption of the haemocyte immune functions. Sci Rep 6:34996. https://doi.org/10.1038/srep34996

Xiao YT, Zhang T, Liu DX, Heckel DG (2014) Mis-splicing of the ABCC2 gene linked with Bt toxin resistance in *Helicoverpa armigera*. Sci Rep 4:6184. https://doi.org/10.1038/srep06184

Yang Q, Zhang J, Li TH, Liu S (2017) PirAB protein from *Xenorhabdus nematophila* HB310 exhibits a binary toxin with insecticidal

activity and cytotoxicity in *Galleria mellonella*. J Invertebr Pathol 148:43–50. https://doi.org/10.1016/j.jip.2017.04.007

Zhou Z, Wang ZY, Liu YX, Liang GM (2016) Identification of ABCC2 as a binding protein of Cry1Ac on brush border membrane vesicles from *Helicoverpa armigera* by an improved pull-down assay. Microbiol Open 5:659–669. https://doi.org/10.1002/mbo3.360

Zúñiga-Navarrete F, Gómez I, Peña G, Bravo A (2013) A *Tenebrio molitor* GPI-anchored alkaline phosphatase is involved in binding of *Bacillus thuringiensis* Cry3Aa to brush border membrane vesicles. Peptides 41:81–86. https://doi.org/10.1016/j.peptides.2012.05.019

Affiliations

Ziyan NanGong[1] · Xiaoxiao Guo[1] · Qing Yang[2] · Ping Song[1] · Qinying Wang[1] · Megha N. Parajulee[3]

✉ Ziyan NanGong
ngzyheb@163.com

[1] Plant Protection College, Hebei Agricultural University, Baoding 071000, China

[2] College of Horticulture and Plant Protection, Yangzhou University, Yangzhou 225009, China

[3] Texas A&M AgriLife Research and Extension Center, Lubbock, TX 79403, USA